



# Advances in the Ritz formulation for free vibration response of doubly-curved anisotropic laminated composite shallow and deep shells

Fiorenzo A. Fazzolari<sup>a,\*</sup>, Erasmo Carrera<sup>b,2</sup>

<sup>a</sup> City University London, Northampton Square, London EC1V 0HB, United Kingdom

<sup>b</sup> Politecnico di Torino, Corso Duca degli Abruzzi 24, 10129 Torino, Italy

## ARTICLE INFO

### Article history:

Available online 8 February 2013

### Keywords:

Advanced hierarchical shell theories  
Doubly-curved anisotropic laminated shells  
Ritz method  
Free vibration

## ABSTRACT

The hierarchical trigonometric Ritz formulation (HTRF) developed in the framework of the Carrera unified formulation (CUF), for the first time, is extended to shell structures in order to cope with the free vibration response of doubly-curved anisotropic laminated composite shells. The HTRF is the outcome of the combination of advanced shell theories hierarchically generated via the CUF with the trigonometric Ritz method. It is based on so-called Ritz fundamental primary nuclei obtained by virtue of the principle of virtual displacements (PVD). The PVD is further used to derive the governing differential equations and natural boundary conditions. Donnell–Mushtari's shallow shell-type equations are given as a particular condition. Several shell geometries accounting for thin and thick shallow cylindrical and spherical shells, deep cylindrical shells and hollow circular cylindrical shells, with cross-ply and angle-ply stacking sequences are investigated. CUF-based refined shell models are assessed by comparison with the 3D elasticity solution. Convergence and accuracy of the presented formulation are examined. The effects of significant parameters such as stacking sequence, length-to-thickness ratio and radius-to-length ratio on the circular frequency parameters are discussed.

© 2013 Elsevier Ltd. All rights reserved.

## 1. Introduction

Shell Structures are widely used in common aerospace applications and an accurate evaluation of their static and dynamic behavior is required in order to provide reliable data to design engineers. They have been researched for many years due to his high stiffness-to-weight and strength-to-weight ratios. During the years many theories have been developed to accurately analyze the static and dynamic behavior of doubly-curved shell structures such as those provided by Donnell [1,2], Mushtari [3,4], Love [5,6], Timoshenko [7], Gol'denveizer [8], Novozhilov [9], Flügge [10,11], Lur'ye [12], Byrne [13], Reissner [14], Naghdy-Berry [15], Sanders [16] and Vlasov [17,18] others were obtained expressly for circular cylindrical shells such as Arnold and Warburton [19,20] and Houghton and Johns [21] (see Leissa [22] for further details). Always within the framework of the shell theories it was pointed out by Koiter [23] (Koiter's recommendation (KR)), that for traditional isotropic one-layer, “refinements of Love's first approximation theory are meaningless unless the effects of transverse shear and normal stresses are both taken into account in a refined theory”. Carrera

[24] amended the KR extending it to composite structures by proposing the following statement: “any refinements of classical models are meaningless, in general, unless the effects of interlaminar continuous transverse shear and normal stresses (strains) are both taken into account in a multilayered shell theory”. The same author [25–29] proposed a unified formulation able to generate a wide class of 2D and quasi-3D equivalent single layer, zig-zag and layer-wise shell models which accurately describe the free vibration behavior of doubly-curved laminated composite shells. Both the axiomatic and the asymptotic-like [30,31] approaches have been embedded in the CUF. The capability to study the effectiveness of each single term in the displacement field independently from its location has been investigated both to vibration [30] and bending [31] analyses. Comprehensive documentations on shell structures can be found in many published papers. Reviews on finite element shell formulations have been given by Denis and Palazzotto [32] and Di and Ramm [33]. Exhaustive reviews on classical theories can be found in Bert [34] and Librescu [35]. Theories regarding to the fulfillment of the  $C_z^0$ -requirements were reviewed by Grigolyuk and Kulikov [36]. As many articles on the application of asymptotic methods have been collected by Fettahlioglu and Steel [37], Widera and Logan [38], Widera and Fan [39], Spencer et al. [40] and Cicala [41]. A complete overview of different problems related to multilayered shells modeling has been provided by Kapania [42] and Noor and Burton [43]. From the huge literature presents on this

\* Corresponding author. Tel.: +44 (0)2070408483; fax: +44 (0)2070408566.

E-mail address: [Fiorenzo.Fazzolari.1@city.ac.uk](mailto:Fiorenzo.Fazzolari.1@city.ac.uk) (F.A. Fazzolari).

<sup>1</sup> Ph.D. Candidate, School of Engineering and Mathematical Sciences.

<sup>2</sup> Professor, Department of Mechanical and Aerospace Engineering.

subject only few attempts have been made in order to solve the governing differential equations in an exact way, Forsberg [44] by using the Donnell and Flügge assumptions and Soedel [45] for orthotropic circular cylindrical shells and simply supported (shear diaphragms) boundary condition, amongst others [46,47]. A systematic procedure for obtaining the closed-form eigensolution was given by Callahan and Baruh [48]. Recently, an analytical procedure to obtain the exact characteristic equation for free vibration analysis of circular cylindrical shells has been given by Liu et al. [49]. Although most of them are based on strong simplifications, these efforts are however necessary due to the high variability with which the approximate solutions match the exact one. Approximate solutions are strongly used in the analysis of shell structures. Zhao et al. [50] used a mesh-free kp-Ritz method for the analysis of laminated cylindrical panels with two side simply-supported. The same author [51] employed a meshfree approach to undertake a free vibration analysis of composite cylindrical panels. Liew and Lim [52] dealt with the vibration analysis of doubly-curved rectangular shallow shells via the Ritz method and a refined first order theory. Lim and Liew [53] used a higher order theory for the free vibration analysis of cylindrical shallow shells. Soldatos and Messina [54] studied the influence of boundary conditions and transverse shear on the free vibration behavior of symmetric and antisymmetric angle-ply laminated circular cylinders and cylindrical panels by a Ritz formulation. Messina and Soldatos [55] investigated the effect of different boundary conditions on the dynamic characteristics of cross-ply laminated circular cylinders. Accurate equations based on the FSDT were provided by Qatu [56] for laminated composite deep thick shells. Qatu and Asadi [57] addressed the vibration analysis of doubly-curved shallow shells with arbitrary boundary conditions by using the Ritz method with algebraic polynomial displacement functions. Asadi et al. [58] employed a 3D and several shear deformation theories in order to carry out static and vibration analysis of thick deep laminated cylindrical shells. Ferreira et al. [59] used a wavelet collocation method for the analysis of laminated shells. The same author [60] combined a sinusoidal shear deformation theory with the radial basis functions collocation method to deal with static and vibration analyses of laminated composite shells. Tornabene [61] studied the free vibration behavior of doubly-curved anisotropic laminated composite shells and revolution panels by means of the generalized differential quadrature (GDQ). Recently some reviews on the recent research on the analysis of composite shells have been presented. Qatu [62] reviews most of the research done on the dynamic behavior of composite shells including free vibration, impact, transient, shock, etc. Liew et al. [63] proposed a review of meshless methods for laminated and functionally graded plates and shells. In the present article the hierarchical trigonometric Ritz formulation (HTRF), which was introduced for the first time by Fazzolari and Carrera in [30,64–67] in order to investigate the static and dynamic behavior of anisotropic laminated composite and sandwich plates, has been extended to shell structures. The trigonometric Ritz method is used in conjunction with the advanced hierarchical shell models provided by the CUF to cope with free vibration analysis of doubly-curved anisotropic laminated composite shells. In the particular case of layer-wise shell models, being the governing differential equations written at layer level a further refinement has been introduced in order to accurately describe the reference surfaces at each layer. However, on the other hand, a refinement in results cannot be achieved only by virtue of an enhancement in the kinematics description of the displacement model, but combining it with an adequate description of the curvature terms  $h/R_i$  with  $i = \alpha, \beta$ . The accuracy of the presented formulation has been widely demonstrated in the results Section 7 by means of several numerical benchmarks. Different shell configurations have been accounted for. An accurate convergence analysis has been carried

out evaluating the effect of the kinematics descriptions and higher order terms on the rate of convergence. In particular, thin and thick shallow cylindrical and spherical shells, deep cylindrical shells and hollow circular cylindrical shells, with cross-ply and angle-ply stacking sequences have been investigated. Some reliable benchmarks have been provided and the effects of key parameters such as stacking sequence, length-to-thickness ratio and radius-to-length ratio on the circular frequency parameters have been commented.

## 2. Laminated composite shell geometries

The salient features of laminated composite shell geometries are shown in Fig. 1. A laminated shell composed of  $N_l$  layers is considered. The integer  $k$ , used as superscript or subscript, denotes the layer number which starts from the bottom of the shell. The layer geometry is denoted by the same symbols as those used for the whole multilayered shell and vice versa. With  $\alpha_k$  and  $\beta_k$  the curvilinear orthogonal coordinates (coinciding with the lines of principal curvature) on the layer reference surface  $\Omega_k$  (middle surface of the  $k$  layer). The  $z_k$  denotes the rectilinear coordinate in the normal direction with respect to the layer middle surface  $\Omega_k$ . The angle  $\phi$  is commonly referred to as shallowness angle. The  $\Gamma_k$  is the  $\Omega_k$  boundary:  $\Gamma_k^g$  and  $\Gamma_k^m$  are those parts of  $\Gamma_k$  on which the geometrical and mechanical boundary conditions are imposed, respectively. These boundaries are herein considered parallel to  $\alpha_k$  or  $\beta_k$ . For convenience the further dimensionless thickness coordinate is introduced  $\zeta_k = \frac{z_k}{h_k}$ , where  $h_k$  denotes the thickness in  $A_k$  domain. The following relationships hold in the given orthogonal system of curvilinear coordinates [68,69]:

- Square of line elements

$$ds_k^2 = \left(H_\alpha^k\right)^2 d\alpha_k^2 + \left(H_\beta^k\right)^2 d\beta_k^2 + \left(H_z^k\right)^2 dz_k^2 \quad (1)$$

- Area of an infinitesimal rectangle on  $\Omega_k$

$$d\Omega_k = H_\alpha^k H_\beta^k d\alpha_k d\beta_k \quad (2)$$

- Infinitesimal volume

$$dV_k = H_\alpha^k H_\beta^k H_z^k d\alpha_k d\beta_k dz_k \quad (3)$$

where

$$H_\alpha^k = A^k \left(1 + \frac{z_k}{R_\alpha^k}\right) \quad H_\beta^k = B^k \left(1 + \frac{z_k}{R_\beta^k}\right) \quad H_z^k = 1 \quad (4)$$

The  $R_\alpha^k$  and  $R_\beta^k$  are the radii of curvature in the  $\alpha_k$  and  $\beta_k$  directions, respectively. The coefficient of the first fundamental form of  $d\Omega_k$  are  $A^k$  and  $B^k$ . Attention is herein focused on shells with a constant curvature, i.e., doubly-curved shells (cylindrical, spherical, toroidal geometries) for which  $A^k = B^k = 1$ .

## 3. Constitutive equations and geometrical relationships

The notation for the displacement vector is:

$$\mathbf{u} = [u_\alpha \quad u_\beta \quad u_z]^T \quad (5)$$

Superscript  $T$  represents the transposition operator. The stresses,  $\boldsymbol{\sigma}$ , and the strains,  $\boldsymbol{\varepsilon}$ , are expressed as follows:

$$\boldsymbol{\sigma}_{\rho H}^k = \begin{bmatrix} \sigma_{\alpha\alpha}^k & \sigma_{\beta\beta}^k & \tau_{\alpha\beta}^k \end{bmatrix}^T, \quad \boldsymbol{\varepsilon}_{pG}^k = \begin{bmatrix} \varepsilon_{\alpha\alpha}^k & \varepsilon_{\beta\beta}^k & \gamma_{\alpha\beta}^k \end{bmatrix}^T \\ \boldsymbol{\sigma}_{nH}^k = \begin{bmatrix} \tau_{\alpha z}^k & \tau_{\beta z}^k & \sigma_{zz}^k \end{bmatrix}^T, \quad \boldsymbol{\varepsilon}_{nG}^k = \begin{bmatrix} \gamma_{\alpha z}^k & \gamma_{\beta z}^k & \varepsilon_{zz}^k \end{bmatrix}^T \quad (6)$$

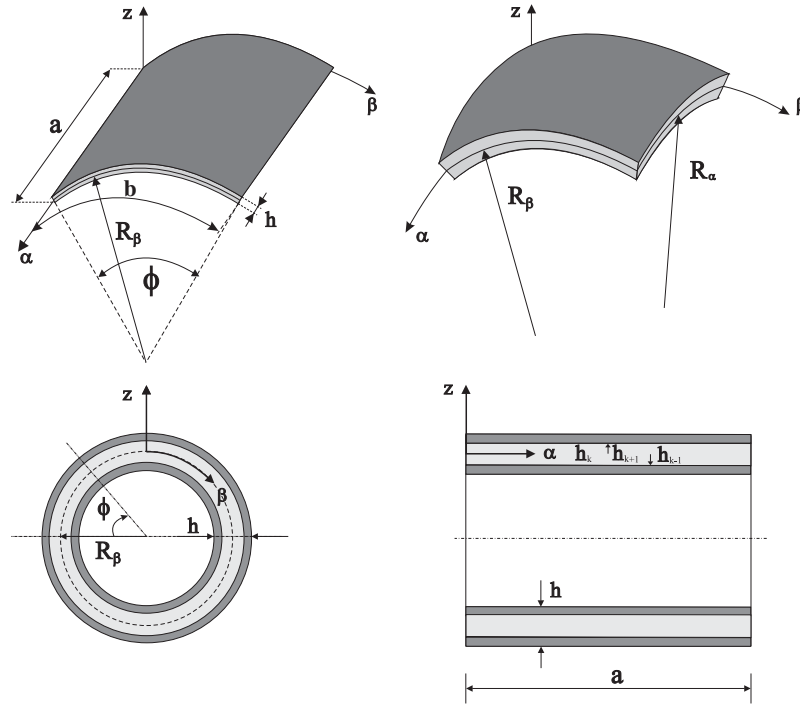


Fig. 1. Laminated composite singly and doubly curved shells.

The subscripts  $n$  and  $p$  denote transverse (out-of-plane, normal), respectively, whilst the subscript  $H$  and  $G$  state that Hooke's law and geometric relations are used. The strain–displacement relations are:

$$\begin{aligned} \boldsymbol{\varepsilon}_{pG}^k &= \mathbf{D}_p \mathbf{u}^k + \mathbf{A}_p \mathbf{u}^k \\ \boldsymbol{\varepsilon}_{nG}^k &= \mathbf{D}_n \mathbf{u}^k + \delta_D \mathbf{A}_n \mathbf{u}^k = \mathbf{D}_{np} \mathbf{u}^k + \delta_D \mathbf{A}_n \mathbf{u}^k + \mathbf{D}_{nz} \mathbf{u}^k \end{aligned} \quad (7)$$

where  $\delta_D$  is a tracer used to introduce Donnell–Mushtari's shallow shell-type approximation,  $\mathbf{D}_p$ ,  $\mathbf{D}_{np}$  and  $\mathbf{D}_{nz}$  are differential matrix operators:

$$\begin{aligned} \mathbf{D}_p &= \begin{bmatrix} \frac{\partial}{\partial z} & 0 & 0 \\ 0 & \frac{\partial}{\partial \beta} & 0 \\ \frac{\partial}{\partial \beta} & \frac{\partial}{\partial \alpha} & 0 \end{bmatrix}, \quad \mathbf{D}_n = \begin{bmatrix} \frac{\partial}{\partial z} & 0 & \frac{\partial}{\partial \alpha} \\ 0 & \frac{\partial}{\partial z} & \frac{\partial}{\partial \beta} \\ 0 & 0 & \frac{\partial}{\partial z} \end{bmatrix}, \\ \mathbf{D}_{np} &= \begin{bmatrix} 0 & 0 & \frac{\partial}{\partial \alpha} \\ 0 & 0 & \frac{\partial}{\partial \beta} \\ 0 & 0 & 0 \end{bmatrix}, \quad \mathbf{D}_{nz} = \begin{bmatrix} \frac{\partial}{\partial z} & 0 & 0 \\ 0 & \frac{\partial}{\partial z} & 0 \\ 0 & 0 & \frac{\partial}{\partial z} \end{bmatrix} \end{aligned} \quad (8)$$

$\mathbf{A}_p$  and  $\mathbf{A}_n$  are matrices containing geometrical parameters operators:

$$\mathbf{A}_p = \begin{bmatrix} 0 & 0 & \frac{1}{H_z^k R_z^k} \\ 0 & 0 & \frac{1}{H_\beta^k R_\beta^k} \\ 0 & 0 & 0 \end{bmatrix}, \quad \mathbf{A}_n = \begin{bmatrix} -\frac{1}{H_z^k R_z^k} & 0 & 0 \\ 0 & -\frac{1}{H_\beta^k R_\beta^k} & 0 \\ 0 & 0 & 0 \end{bmatrix} \quad (9)$$

In the case of orthotropic materials, Hooke's law holds:

$$\boldsymbol{\sigma}^k = \mathbf{C}^k \boldsymbol{\varepsilon}^k \quad (10)$$

According to Eq. (6), the previous equation becomes:

$$\begin{aligned} \boldsymbol{\sigma}_{pH}^k &= \tilde{\mathbf{C}}_{pp}^k \boldsymbol{\varepsilon}_{pG}^k + \tilde{\mathbf{C}}_{pn}^k \boldsymbol{\varepsilon}_{nG}^k \\ \boldsymbol{\sigma}_{nH}^k &= \tilde{\mathbf{C}}_{np}^k \boldsymbol{\varepsilon}_{pG}^k + \tilde{\mathbf{C}}_{nn}^k \boldsymbol{\varepsilon}_{nG}^k \end{aligned} \quad (11)$$

where matrices  $\tilde{\mathbf{C}}_{pp}^k$ ,  $\tilde{\mathbf{C}}_{nn}^k$ ,  $\tilde{\mathbf{C}}_{pn}^k$  and  $\tilde{\mathbf{C}}_{np}^k$  are:

$$\begin{aligned} \tilde{\mathbf{C}}_{pp}^k &= \begin{bmatrix} \tilde{C}_{11} & \tilde{C}_{12} & \tilde{C}_{16} \\ \tilde{C}_{12} & \tilde{C}_{22} & \tilde{C}_{26} \\ \tilde{C}_{16} & \tilde{C}_{26} & \tilde{C}_{66} \end{bmatrix}^k, \quad \tilde{\mathbf{C}}_{nn}^k = \begin{bmatrix} \tilde{C}_{55} & \tilde{C}_{45} & 0 \\ \tilde{C}_{45} & \tilde{C}_{44} & 0 \\ 0 & 0 & \tilde{C}_{33} \end{bmatrix}^k, \\ \tilde{\mathbf{C}}_{pn}^k &= \begin{bmatrix} 0 & 0 & \tilde{C}_{13} \\ 0 & 0 & \tilde{C}_{23} \\ 0 & 0 & \tilde{C}_{36} \end{bmatrix}^k, \quad \tilde{\mathbf{C}}_{np}^k = \begin{bmatrix} 0 & 0 & 0 \\ 0 & 0 & 0 \\ \tilde{C}_{13} & \tilde{C}_{23} & \tilde{C}_{36} \end{bmatrix}^k \end{aligned} \quad (12)$$

and are expressed in the laminate coordinate system following the stress tensor transformation rule. For the sake of conciseness, the dependence of the coefficients  $\tilde{C}_{ij}$  versus Young's moduli, Poisson's ratio, the shear moduli and the fiber angle is not reported. It can be found in Tsai [70], Reddy [71] or Jones [72].

#### 4. Advanced and refined hierarchical shell models

The theories of thin shells which are commonly used are based on the assumption that the transverse normal stress may be neglected in the material constitutive equations. This assumption is substantiated by the fact that in usual applications in-plane stresses have generally bigger of magnitude. Furthermore from Love's hypothesis the transverse normal strain is zero. However these assumptions are no longer valid when 3D local effects appear. Consequently, as highlighted in [73], a theory which includes  $\sigma_{zz} = 0$  and  $\varepsilon_{zz} = 0$  leads to wrong results. To remove the inconsistency completely, it is compulsory to expand the displacement field at higher order with respect to the  $z$  coordinate. According to the above considerations the CUF, well known in the static and dynamics analysis of layered beams, plates and shells, removes the inconsistency generating a large variety of 2D and quasi-3D hierarchical models using a unified approach. According to the CUF, weak and strong formulations of the governing differential equations are written in terms of primary fundamental nuclei, which are mathematically and formally independent both from the expansion orders used in the displacement field for each unknown variable and from the used kinematics description such as equivalent single

layer, zig-zag or layer-wise. Moreover, in the case of weak formulation the Ritz primary fundamental nuclei are invariant with respect to the chosen trial functions. By using an axiomatic approach, the problem related to the shell structures can be reduced from 3D to 2D. Mathematically, this means that, the unknown variables can be expressed as a set of thickness functions that only depend on the thickness coordinate  $z$  (or  $\zeta^k$  in the case of layer-wise shell theories) and the associated variable depending on the in-plane orthogonal curvilinear coordinates  $\alpha$  and  $\beta$ . The capability to use different expansion orders  $N_{u_\alpha}$ ,  $N_{u_\beta}$  and  $N_{u_z}$  in the thickness-shell-direction for each unknown variable in the displacement field [30,74–80] is included in the presented shell models. Such artifice permits to treat each variable independently from the others and this becomes extremely useful when multifield analyses are carried out such as in thermo-elastic [66,74] and piezoelectric [81] applications. Therefore, following this approach the displacement variables can be written in compact form as:

$$\mathbf{u}^k = \mathbf{F}_\tau \mathbf{u}_\tau^k, \quad \tau = \tau_{u_\alpha}, \tau_{u_\beta}, \tau_{u_z} \tag{13}$$

and their virtual variation:

$$\delta \mathbf{u}^k = \mathbf{F}_s \delta \mathbf{u}_s^k, \quad s = s_{u_\alpha}, s_{u_\beta}, s_{u_z} \tag{14}$$

where

$$\mathbf{F}_\tau = \begin{bmatrix} F_{\tau_{u_\alpha}} & 0 & 0 \\ 0 & F_{\tau_{u_\beta}} & 0 \\ 0 & 0 & F_{\tau_{u_z}} \end{bmatrix}, \quad \mathbf{u}_\tau^k = \begin{bmatrix} u_{\alpha\tau_{u_\alpha}} \\ u_{\beta\tau_{u_\beta}} \\ u_{z\tau_{u_z}} \end{bmatrix}^k, \quad \delta \mathbf{u}_\tau^k = \begin{bmatrix} \delta u_{\alpha\tau_{u_\alpha}} \\ \delta u_{\beta\tau_{u_\beta}} \\ \delta u_{z\tau_{u_z}} \end{bmatrix}^k \tag{15}$$

$F_{\tau_{u_\alpha}}, F_{\tau_{u_\beta}}, F_{\tau_{u_z}}$  are functions of  $z$ . The axiomatic hierarchical shell models here employed are based on the chosen of polynomials which are introduced by the aforementioned thickness functions and describe the trend of the displacement components through the thickness-shell-direction. The functions  $u_{\alpha\tau_{u_\alpha}}, u_{\beta\tau_{u_\beta}}, u_{z\tau_{u_z}}$  are displacement vectors. According to Einstein's notation, the repeated subscripts  $\tau_{u_\alpha}, \tau_{u_\beta}, \tau_{u_z}$  indicate summation. Since superscript  $k$  appears in the primary unknown variables a layer-wise kinematics description is implied. The thickness functions  $F_{\tau_{u_\alpha}}(\zeta_k), F_{\tau_{u_\beta}}(\zeta_k), F_{\tau_{u_z}}(\zeta_k)$  have now been defined at the  $k$ -layer level as follows:

$$\begin{aligned} F_{t_{u_\alpha}} &= \frac{P_0 + P_1}{2}, & F_{b_{u_\alpha}} &= \frac{P_0 - P_1}{2}, & F_{r_{u_\alpha}} &= P_{r_{u_\alpha}} - P_{r_{u_\alpha}-2}, \\ r_{u_\alpha} &= 1, 2, 3, \dots, N_{u_\alpha} - 1 \\ F_{t_{u_\beta}} &= \frac{P_0 + P_1}{2}, & F_{b_{u_\beta}} &= \frac{P_0 - P_1}{2}, & F_{r_{u_\beta}} &= P_{r_{u_\beta}} - P_{r_{u_\beta}-2}, \\ r_{u_\beta} &= 1, 2, 3, \dots, N_{u_\beta} - 1 \\ F_{t_{u_z}} &= \frac{P_0 + P_1}{2}, & F_{b_{u_z}} &= \frac{P_0 - P_1}{2}, & F_{r_{u_z}} &= P_{r_{u_z}} - P_{r_{u_z}-2}, \\ r_{u_z} &= 1, 2, 3, \dots, N_{u_z} - 1 \end{aligned} \tag{16}$$

where subscript  $t$  and  $b$  refer to the layer top and bottom respectively, furthermore the  $P_j = P_j(\zeta_k)$  is the Legendre polynomial of the  $j$ -order defined in the  $\zeta_k$ -domain:  $-1 \leq \zeta_k \leq 1$ . A parabolic displacement field is shown in Fig. 2. The related polynomials are:

$$\begin{aligned} P_0 &= 1, & P_1 &= \zeta_k, & P_2 &= \frac{3\zeta_k - 1}{2}, & P_3 &= \frac{5\zeta_k^3 - 3\zeta_k}{2}, & P_4 &= \\ &= \frac{35\zeta_k^4 - 15\zeta_k^2 + 3}{8}, & P_5 &= \frac{63\zeta_k^5 - 35\zeta_k^3 + 15\zeta_k}{8} \end{aligned} \tag{17}$$

The chosen functions have the following properties:

$$\zeta_k = \begin{cases} 1 : & F_{b_{u_\alpha}}, F_{b_{u_\beta}}, F_{b_{u_z}} = 0; & F_{r_{u_\alpha}}, F_{r_{u_\beta}}, F_{r_{u_z}} = 0; & F_{t_{u_\alpha}}, F_{t_{u_\beta}}, F_{t_{u_z}} = 1; \\ -1 : & F_{b_{u_\alpha}}, F_{b_{u_\beta}}, F_{b_{u_z}} = 1; & F_{r_{u_\alpha}}, F_{r_{u_\beta}}, F_{r_{u_z}} = 0; & F_{t_{u_\alpha}}, F_{t_{u_\beta}}, F_{t_{u_z}} = 0; \end{cases} \tag{18}$$

The top and bottom values have been used as unknown variables. The interlaminar compatibility of displacements at each interface is easily linked:

$$u_{t_{u_\alpha}}^k = u_{b_{u_\alpha}}^{k+1}, \quad u_{t_{u_\beta}}^k = u_{b_{u_\beta}}^{k+1}, \quad u_{t_{u_z}}^k = u_{b_{u_z}}^{k+1}, \quad k = 1, \dots, N_l - 1 \tag{19}$$

However, on the other hand, it is possible to employ an equivalent single layer approach for the primary displacement variables, in that case the thickness functions are expressed in Taylor series and using the same notation adopted in the layer-wise case, the thickness functions are written as follows:

$$\begin{aligned} F_{b_{u_\alpha}} &= 1, & F_{r_{u_\alpha}} &= z^{r_{u_\alpha}}, & F_{t_{u_\alpha}} &= z^{N_{u_\alpha}}, & r_{u_\alpha} &= 1, 2, 3, \dots, N_{u_\alpha} - 1 \\ F_{b_{u_\beta}} &= 1, & F_{r_{u_\beta}} &= z^{r_{u_\beta}}, & F_{t_{u_\beta}} &= z^{N_{u_\beta}}, & r_{u_\beta} &= 1, 2, 3, \dots, N_{u_\beta} - 1 \\ F_{b_{u_z}} &= 1, & F_{r_{u_z}} &= z^{r_{u_z}}, & F_{t_{u_z}} &= z^{N_{u_z}}, & r_{u_z} &= 1, 2, 3, \dots, N_{u_z} - 1 \end{aligned} \tag{20}$$

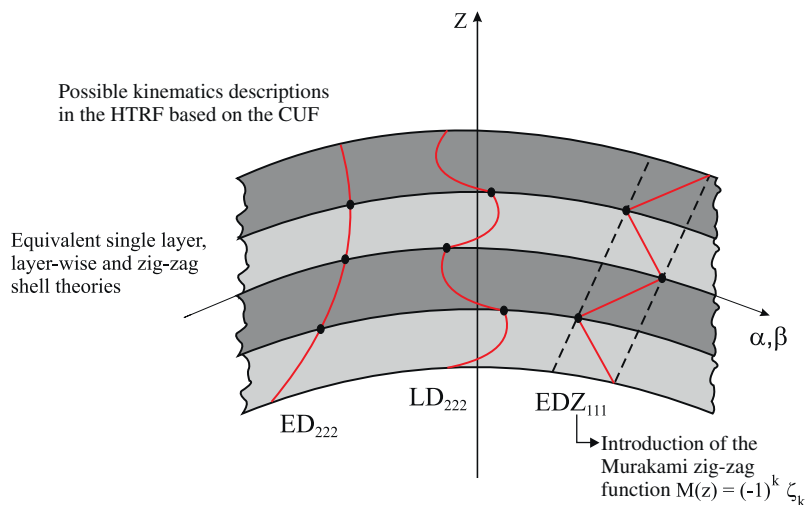


Fig. 2. Advanced shell models.

A parabolic displacement field is shown in Fig. 2. Nevertheless, it should bear in mind that equivalent single layer models violate interlaminar equilibrium of transverse stresses and they do not describe the zig-zag trend of the displacement components in the thickness direction. Nonetheless, the zig-zag trends which hinges on the transverse anisotropy of composite structures, can be accounted for in the equivalent single layer shell models by simply adding the Murakami zig-zag function (MZZF),  $M(z) = (-1)^k \zeta_k$ , which reproduces the discontinuity of the first derivative of the displacement variables in the z-direction, and the displacement field in Eq. (20) becomes,

$$\begin{aligned} F_{b_{u_x}} &= 1, & F_{r_{u_x}} &= z^{r_{u_x}}, & F_{t_{u_x}} &= (-1)^k \zeta_k, & r_{u_x} &= 1, 2, 3, \dots, N_{u_x} - 1 \\ F_{b_{u_\beta}} &= 1, & F_{r_{u_\beta}} &= z^{r_{u_\beta}}, & F_{t_{u_\beta}} &= (-1)^k \zeta_k, & r_{u_\beta} &= 1, 2, 3, \dots, N_{u_\beta} - 1 \\ F_{b_{u_z}} &= 1, & F_{r_{u_z}} &= z^{r_{u_z}}, & F_{t_{u_z}} &= (-1)^k \zeta_k, & r_{u_z} &= 1, 2, 3, \dots, N_{u_z} - 1 \end{aligned} \quad (21)$$

It should be noticed that  $F_{t_{u_x}}, F_{t_{u_\beta}}, F_{t_{u_z}}$  assume the values  $\pm 1$  in correspondence to the bottom and the top interfaces of the  $k$ -layer (see Fig. 2). An exhaustive and comprehensive documentation on the MZZF can be found in [82–85].

### 5. Theoretical formulation

The variational statement used in the derivation of what follows is the principle of virtual displacements (PVD). The PVD is a powerful tool employed both to develop approximate solution methods and to derive the governing differential equations with natural boundary conditions when applied in conjunction with the Gauss theorem. The explicit form of the PVD at multilayer level, can be written as:

$$\sum_{k=1}^{N_l} \int_{\Omega^k} \int_{A^k} \left( \delta \mathbf{e}_{pG}^{kT} \boldsymbol{\sigma}_{pG}^k + \delta \mathbf{e}_{nG}^{kT} \boldsymbol{\sigma}_{nG}^k \right) d\Omega^k dz = - \sum_{k=1}^{N_l} \delta L_{F_{in}}^k \quad (22)$$

#### 5.1. The hierarchical trigonometric Ritz formulation

The HTRF, herein proposed for doubly-curved shells, is based on the Ritz fundamental primary nuclei, which can be developed following four steps [67]:

1. The choice of the variational statement.
2. The introduction of the stress–strain constitutive relationships.
3. The choice of the Ritz functions.
4. The use of the geometric relations.

The PVD has already been chosen as variational statement (see Eq. (22)), the stress–strain constitutive relationships have been given in Eq. (11). The third step is the definition of the displacement field in terms of Ritz functions. In particular, in the Ritz method the displacement amplitude vector  $\mathbf{u}^k$  is that which individuates the maximum amplitude in the oscillation, that maximizes the related work and is expressed in series expansion as:

$$\mathbf{u}_\tau^k = \mathbf{U}_{\tau i}^k \boldsymbol{\Psi}_i \quad \text{where } i = 1, \dots, \mathcal{N} \quad \tau = \tau_{u_x}, \tau_{u_\beta}, \tau_{u_z} \quad (23)$$

$\mathcal{N}$  indicates the order of expansion in the approximation,  $\iota = \sqrt{-1}$ ,  $t$  is the time and  $\omega_{ij}$  the circular frequency. Consequently the harmonic displacement field, in compact way, assumes the following form:

$$\mathbf{u}^k = \mathbf{F}_\tau \mathbf{U}_{\tau i}^k \boldsymbol{\Psi}_i \quad (24)$$

where

$$\mathbf{U}_{\tau i}^k = \begin{bmatrix} U_{\alpha \tau_{u_x} i}^k e^{\iota \omega_{ij} t} \\ U_{\beta \tau_{u_\beta} i}^k e^{\iota \omega_{ij} t} \\ U_{\gamma \tau_{u_z} i}^k e^{\iota \omega_{ij} t} \end{bmatrix}, \quad \boldsymbol{\Psi}_i = \begin{bmatrix} \psi_{\alpha_i} & 0 & 0 \\ 0 & \psi_{\beta_i} & 0 \\ 0 & 0 & \psi_{\gamma_i} \end{bmatrix}, \quad \mathbf{F}_\tau = \begin{bmatrix} F_{\tau_{u_x}} & 0 & 0 \\ 0 & F_{\tau_{u_\beta}} & 0 \\ 0 & 0 & F_{\tau_{u_z}} \end{bmatrix} \quad (25)$$

$U_{\alpha \tau_{u_x} i}^k, U_{\beta \tau_{u_\beta} i}^k, U_{\gamma \tau_{u_z} i}^k$  are the unknown coefficients,  $\psi_{\alpha_i}, \psi_{\beta_i}, \psi_{\gamma_i}$  are the Ritz functions appropriately chosen on the type of problem. Convergence to the exact solution is guaranteed if the basis functions are admissible functions in the used variational principle [64,86,87]. In the fourth step, by coupling the geometrical relations in Eq. (7) with Eq. (24) the strain vectors become:

$$\begin{aligned} \mathbf{e}_{pG}^k &= \mathbf{D}_p(\mathbf{F}_\tau \boldsymbol{\Psi}_i) \mathbf{U}_{\tau i}^k + \mathbf{A}_p(\mathbf{F}_\tau \boldsymbol{\Psi}_i) \mathbf{U}_{\tau i}^k \\ \mathbf{e}_{nG}^k &= \mathbf{D}_{np}(\mathbf{F}_\tau \boldsymbol{\Psi}_i) \mathbf{U}_{\tau i}^k + \delta_D \mathbf{A}_n(\mathbf{F}_\tau \boldsymbol{\Psi}_i) \mathbf{U}_{\tau i}^k + \mathbf{D}_{nz}(\mathbf{F}_\tau \boldsymbol{\Psi}_i) \mathbf{U}_{\tau i}^k \end{aligned} \quad (26)$$

By substituting the previous expression in Eq. (22) the explicit expressions of the internal work and the work done by the inertial forces in terms of Ritz functions and unknown coefficients are obtained:

$$\begin{aligned} \delta L_{int}^k &= \int_{\Omega_k} \int_{A^k} \delta \mathbf{U}_{\tau i}^{kT} [\mathbf{D}_p(\mathbf{F}_\tau \boldsymbol{\Psi}_i)]^T \tilde{\mathbf{C}}_{pp}^k \mathbf{D}_p(\mathbf{F}_s \boldsymbol{\Psi}_j) \mathbf{U}_{s j}^k d\Omega_k dz + \\ &\int_{\Omega_k} \int_{A^k} \delta \mathbf{U}_{\tau i}^{kT} [\mathbf{D}_p(\mathbf{F}_\tau \boldsymbol{\Psi}_i)]^T \tilde{\mathbf{C}}_{pp}^k \mathbf{A}_p(\mathbf{F}_s \boldsymbol{\Psi}_j) \mathbf{U}_{s j}^k d\Omega_k dz + \\ &\int_{\Omega_k} \int_{A^k} \delta \mathbf{U}_{\tau i}^{kT} [\mathbf{D}_p(\mathbf{F}_\tau \boldsymbol{\Psi}_i)]^T \tilde{\mathbf{C}}_{pn}^k \mathbf{D}_{np}(\mathbf{F}_s \boldsymbol{\Psi}_j) \mathbf{U}_{s j}^k d\Omega_k dz + \\ &\int_{\Omega_k} \int_{A^k} \delta \mathbf{U}_{\tau i}^{kT} [\mathbf{D}_p(\mathbf{F}_\tau \boldsymbol{\Psi}_i)]^T \tilde{\mathbf{C}}_{pn}^k \delta_D \mathbf{A}_n(\mathbf{F}_s \boldsymbol{\Psi}_j) \mathbf{U}_{s j}^k d\Omega_k dz + \\ &\int_{\Omega_k} \int_{A^k} \delta \mathbf{U}_{\tau i}^{kT} [\mathbf{D}_p(\mathbf{F}_\tau \boldsymbol{\Psi}_i)]^T \tilde{\mathbf{C}}_{pn}^k \mathbf{D}_{nz}(\mathbf{F}_s \boldsymbol{\Psi}_j) \mathbf{U}_{s j}^k d\Omega_k dz + \\ &\int_{\Omega_k} \int_{A^k} \delta \mathbf{U}_{\tau i}^{kT} [\mathbf{A}_p(\mathbf{F}_\tau \boldsymbol{\Psi}_i)]^T \tilde{\mathbf{C}}_{pp}^k \mathbf{D}_p(\mathbf{F}_s \boldsymbol{\Psi}_j) \mathbf{U}_{s j}^k d\Omega_k dz + \\ &\int_{\Omega_k} \int_{A^k} \delta \mathbf{U}_{\tau i}^{kT} [\mathbf{A}_p(\mathbf{F}_\tau \boldsymbol{\Psi}_i)]^T \tilde{\mathbf{C}}_{pp}^k \mathbf{A}_p(\mathbf{F}_s \boldsymbol{\Psi}_j) \mathbf{U}_{s j}^k d\Omega_k dz + \\ &\int_{\Omega_k} \int_{A^k} \delta \mathbf{U}_{\tau i}^{kT} [\mathbf{A}_p(\mathbf{F}_\tau \boldsymbol{\Psi}_i)]^T \tilde{\mathbf{C}}_{pn}^k \mathbf{D}_{np}(\mathbf{F}_s \boldsymbol{\Psi}_j) \mathbf{U}_{s j}^k d\Omega_k dz + \\ &\int_{\Omega_k} \int_{A^k} \delta \mathbf{U}_{\tau i}^{kT} [\mathbf{A}_p(\mathbf{F}_\tau \boldsymbol{\Psi}_i)]^T \tilde{\mathbf{C}}_{pn}^k \delta_D \mathbf{A}_n(\mathbf{F}_s \boldsymbol{\Psi}_j) \mathbf{U}_{s j}^k d\Omega_k dz + \\ &\int_{\Omega_k} \int_{A^k} \delta \mathbf{U}_{\tau i}^{kT} [\mathbf{A}_p(\mathbf{F}_\tau \boldsymbol{\Psi}_i)]^T \tilde{\mathbf{C}}_{pn}^k \mathbf{D}_{nz}(\mathbf{F}_s \boldsymbol{\Psi}_j) \mathbf{U}_{s j}^k d\Omega_k dz + \\ &\int_{\Omega_k} \int_{A^k} \delta \mathbf{U}_{\tau i}^{kT} [\mathbf{D}_{np}(\mathbf{F}_\tau \boldsymbol{\Psi}_i)]^T \tilde{\mathbf{C}}_{np}^k \mathbf{D}_p(\mathbf{F}_s \boldsymbol{\Psi}_j) \mathbf{U}_{s j}^k d\Omega_k dz + \\ &\int_{\Omega_k} \int_{A^k} \delta \mathbf{U}_{\tau i}^{kT} [\mathbf{D}_{np}(\mathbf{F}_\tau \boldsymbol{\Psi}_i)]^T \tilde{\mathbf{C}}_{np}^k \mathbf{A}_p(\mathbf{F}_s \boldsymbol{\Psi}_j) \mathbf{U}_{s j}^k d\Omega_k dz + \\ &\int_{\Omega_k} \int_{A^k} \delta \mathbf{U}_{\tau i}^{kT} [\mathbf{D}_{np}(\mathbf{F}_\tau \boldsymbol{\Psi}_i)]^T \tilde{\mathbf{C}}_{nn}^k \mathbf{D}_{np}(\mathbf{F}_s \boldsymbol{\Psi}_j) \mathbf{U}_{s j}^k d\Omega_k dz + \\ &\int_{\Omega_k} \int_{A^k} \delta \mathbf{U}_{\tau i}^{kT} [\mathbf{D}_{np}(\mathbf{F}_\tau \boldsymbol{\Psi}_i)]^T \tilde{\mathbf{C}}_{nn}^k \delta_D \mathbf{A}_n(\mathbf{F}_s \boldsymbol{\Psi}_j) \mathbf{U}_{s j}^k d\Omega_k dz + \\ &\int_{\Omega_k} \int_{A^k} \delta \mathbf{U}_{\tau i}^{kT} [\mathbf{D}_{np}(\mathbf{F}_\tau \boldsymbol{\Psi}_i)]^T \tilde{\mathbf{C}}_{nn}^k \mathbf{D}_{nz}(\mathbf{F}_s \boldsymbol{\Psi}_j) \mathbf{U}_{s j}^k d\Omega_k dz + \\ &\int_{\Omega_k} \int_{A^k} \delta \mathbf{U}_{\tau i}^{kT} [\delta_D \mathbf{A}_n(\mathbf{F}_\tau \boldsymbol{\Psi}_i)]^T \tilde{\mathbf{C}}_{np}^k \mathbf{D}_p(\mathbf{F}_s \boldsymbol{\Psi}_j) \mathbf{U}_{s j}^k d\Omega_k dz + \\ &\int_{\Omega_k} \int_{A^k} \delta \mathbf{U}_{\tau i}^{kT} [\delta_D \mathbf{A}_n(\mathbf{F}_\tau \boldsymbol{\Psi}_i)]^T \tilde{\mathbf{C}}_{np}^k \mathbf{A}_p(\mathbf{F}_s \boldsymbol{\Psi}_j) \mathbf{U}_{s j}^k d\Omega_k dz + \end{aligned} \quad (27)$$



$$\begin{aligned} & \int_{\Omega_k} \int_{A^k} \delta \mathbf{U}_{\tau i}^{kT} [\delta_D \mathbf{A}_n(\mathbf{F}_\tau \Psi_i)]^T \tilde{\mathbf{C}}_{nn}^k \mathbf{D}_{np}(\mathbf{F}_s \Psi_j) \mathbf{U}_{sj}^k d\Omega_k dz + \\ & \int_{\Omega_k} \int_{A^k} \delta \mathbf{U}_{\tau i}^{kT} [\delta_D \mathbf{A}_n(\mathbf{F}_\tau \Psi_i)]^T \tilde{\mathbf{C}}_{nn}^k \delta_D \mathbf{A}_n(\mathbf{F}_s \Psi_j) \mathbf{U}_{sj}^k d\Omega_k dz + \\ & \int_{\Omega_k} \int_{A^k} \delta \mathbf{U}_{\tau i}^{kT} [\delta_D \mathbf{A}_n(\mathbf{F}_\tau \Psi_i)]^T \tilde{\mathbf{C}}_{nn}^k \mathbf{D}_{nz}(\mathbf{F}_s \Psi_j) \mathbf{U}_{sj}^k d\Omega_k dz + \\ & \int_{\Omega_k} \int_{A^k} \delta \mathbf{U}_{\tau i}^{kT} [\mathbf{D}_{nz}(\mathbf{F}_\tau \Psi_i)]^T \tilde{\mathbf{C}}_{np}^k \mathbf{D}_p(\mathbf{F}_s \Psi_j) \mathbf{U}_{sj}^k d\Omega_k dz + \\ & \int_{\Omega_k} \int_{A^k} \delta \mathbf{U}_{\tau i}^{kT} [\mathbf{D}_{nz}(\mathbf{F}_\tau \Psi_i)]^T \tilde{\mathbf{C}}_{np}^k \mathbf{A}_p(\mathbf{F}_s \Psi_j) \mathbf{U}_{sj}^k d\Omega_k dz + \\ & \int_{\Omega_k} \int_{A^k} \delta \mathbf{U}_{\tau i}^{kT} [\mathbf{D}_{nz}(\mathbf{F}_\tau \Psi_i)]^T \tilde{\mathbf{C}}_{nn}^k \mathbf{D}_{np}(\mathbf{F}_s \Psi_j) \mathbf{U}_{sj}^k d\Omega_k dz + \\ & \int_{\Omega_k} \int_{A^k} \delta \mathbf{U}_{\tau i}^{kT} [\mathbf{D}_{nz}(\mathbf{F}_\tau \Psi_i)]^T \tilde{\mathbf{C}}_{nn}^k \delta_D \mathbf{A}_n(\mathbf{F}_s \Psi_j) \mathbf{U}_{sj}^k d\Omega_k dz + \\ & \int_{\Omega_k} \int_{A^k} \delta \mathbf{U}_{\tau i}^{kT} [\mathbf{D}_{nz}(\mathbf{F}_\tau \Psi_i)]^T \tilde{\mathbf{C}}_{nn}^k \mathbf{D}_{nz}(\mathbf{F}_s \Psi_j) \mathbf{U}_{sj}^k d\Omega_k dz \\ \delta L_{F_{in}}^k &= \int_{\Omega_k} \int_{A^k} \delta \mathbf{U}_{\tau i}^{kT} [\rho^k (\mathbf{F}_\tau \Psi_i)^T (\mathbf{F}_s \Psi_j)] \ddot{\mathbf{U}}_{sj} d\Omega_k dz \end{aligned}$$

The quadratic forms of the internal work and the work done by the inertial forces can be written as:

$$\delta L_{int}^k = \delta \mathbf{U}_{\tau i}^{kT} \mathbf{K}^{k\tau s i j} \mathbf{U}_{sj}^k, \quad \delta L_{F_{in}}^k = \delta \mathbf{U}_{\tau i}^{kT} \mathbf{M}^{k\tau s i j} \ddot{\mathbf{U}}_{sj}^k \quad (28)$$

the Ritz fundamental primary nuclei are easily obtained comparing Eq. (27) with Eq. (28):

$$\begin{aligned} \mathbf{K}^{k\tau s i j} &= \int_{\Omega_k} \int_{A^k} \left( [(\mathbf{D}_p(\mathbf{F}_\tau \Psi_i))^T + (\mathbf{A}_p(\mathbf{F}_\tau \Psi_i))^T] [\tilde{\mathbf{C}}_{pp}^k \mathbf{D}_p(\mathbf{F}_s \Psi_j) \right. \\ &+ \tilde{\mathbf{C}}_{pp}^k \mathbf{A}_p(\mathbf{F}_s \Psi_j) + \tilde{\mathbf{C}}_{pn}^k \mathbf{D}_{np}(\mathbf{F}_s \Psi_j) + \tilde{\mathbf{C}}_{pn}^k \delta_D \mathbf{A}_n(\mathbf{F}_s \Psi_j) \\ &+ \tilde{\mathbf{C}}_{pn}^k \mathbf{D}_{nz}(\mathbf{F}_s \Psi_j)] + [(\mathbf{D}_{np}(\mathbf{F}_\tau \Psi_i))^T + [\delta_D \mathbf{A}_n(\mathbf{F}_\tau \Psi_i)]^T \\ &+ [\mathbf{D}_{nz}(\mathbf{F}_\tau \Psi_i)]^T] [\tilde{\mathbf{C}}_{np}^k \mathbf{D}_p(\mathbf{F}_s \Psi_j) + \tilde{\mathbf{C}}_{np}^k \mathbf{A}_p(\mathbf{F}_s \Psi_j) \\ &+ \tilde{\mathbf{C}}_{nn}^k \mathbf{D}_{np}(\mathbf{F}_s \Psi_j) + \tilde{\mathbf{C}}_{nn}^k \delta_D \mathbf{A}_n(\mathbf{F}_s \Psi_j) + \tilde{\mathbf{C}}_{nn}^k \mathbf{D}_{nz}(\mathbf{F}_s \Psi_j)] \Big) d\Omega_k dz \\ \mathbf{M}^{k\tau s i j} &= \int_{\Omega_k} \int_{A^k} (\rho^k [(\mathbf{F}_\tau \Psi_i)^T (\mathbf{F}_s \Psi_j)]) d\Omega_k dz \quad (29) \end{aligned}$$

At this point it is useful to introduce the following integrals in order to write in a concise manner the explicit form of the Ritz fundamental secondary nuclei:

$$\begin{aligned} (J_{\alpha}^{k\tau s}, J_{\alpha}^{k\tau s}, J_{\beta}^{k\tau s}, J_{\beta}^{k\tau s}, J_{\alpha}^{k\tau s}, J_{\alpha}^{k\tau s}) &= \int_{A^k} F_{\tau} F_s \left( 1, H_{\alpha}^k, H_{\beta}^k, \frac{H_{\alpha}^k}{H_{\beta}^k}, \frac{H_{\beta}^k}{H_{\alpha}^k}, H_{\alpha}^k H_{\beta}^k \right) dz \\ (J_{\alpha}^{k\tau s}, J_{\alpha}^{k\tau s}, J_{\beta}^{k\tau s}, J_{\beta}^{k\tau s}, J_{\alpha}^{k\tau s}, J_{\alpha}^{k\tau s}) &= \int_{A^k} \frac{\partial F_{\tau}}{\partial Z} F_s \left( 1, H_{\alpha}^k, H_{\beta}^k, \frac{H_{\alpha}^k}{H_{\beta}^k}, \frac{H_{\beta}^k}{H_{\alpha}^k}, H_{\alpha}^k H_{\beta}^k \right) dz \\ (J_{\alpha}^{k\tau s}, J_{\alpha}^{k\tau s}, J_{\beta}^{k\tau s}, J_{\beta}^{k\tau s}, J_{\alpha}^{k\tau s}, J_{\alpha}^{k\tau s}) &= \int_{A^k} F_{\tau} \frac{\partial F_s}{\partial Z} \left( 1, H_{\alpha}^k, H_{\beta}^k, \frac{H_{\alpha}^k}{H_{\beta}^k}, \frac{H_{\beta}^k}{H_{\alpha}^k}, H_{\alpha}^k H_{\beta}^k \right) dz \\ (J_{\alpha}^{k\tau s}, J_{\alpha}^{k\tau s}, J_{\beta}^{k\tau s}, J_{\beta}^{k\tau s}, J_{\alpha}^{k\tau s}, J_{\alpha}^{k\tau s}) &= \int_{A^k} \frac{\partial F_{\tau}}{\partial Z} \frac{\partial F_s}{\partial Z} \left( 1, H_{\alpha}^k, H_{\beta}^k, \frac{H_{\alpha}^k}{H_{\beta}^k}, \frac{H_{\beta}^k}{H_{\alpha}^k}, H_{\alpha}^k H_{\beta}^k \right) dz \quad (30) \end{aligned}$$

where  $\tau = \tau_{u_x}, \tau_{u_y}, \tau_{u_z}$  and  $s = s_{u_x}, s_{u_y}, s_{u_z}$ . The explicit forms of the Ritz fundamental secondary stiffness and mass nuclei are following reported:

$$\begin{aligned} K_{u_x u_x}^{\tau_{u_x} s_{u_x}} &= \tilde{C}_{11}^k J_{\frac{\beta}{\alpha}}^k \int_{\Omega^k} (\psi_{\alpha_i, \alpha} \psi_{\beta_j, \alpha}) d\alpha_k d\beta_k \\ &+ \tilde{C}_{16}^k J^k \int_{\Omega^k} (\psi_{\alpha_i, \alpha} \psi_{\beta_j, \beta}) d\alpha_k d\beta_k \\ &+ \tilde{C}_{16}^k J^k \int_{\Omega^k} (\psi_{\alpha_i, \beta} \psi_{\beta_j, \alpha}) d\alpha_k d\beta_k \\ &+ \tilde{C}_{66}^k J_{\frac{\beta}{\alpha}}^k \int_{\Omega^k} (\psi_{\alpha_i, \beta} \psi_{\beta_j, \beta}) d\alpha_k d\beta_k \\ &+ \tilde{C}_{55}^k J_{\alpha \beta}^k \int_{\Omega^k} (\psi_{\alpha_i} \psi_{\beta_j}) d\alpha_k d\beta_k \\ &+ \delta_D \times \left( -\tilde{C}_{55}^k \frac{1}{R_{\beta}^k} J_{\beta}^k \int_{\Omega^k} (\psi_{\alpha_i} \psi_{\beta_j}) d\alpha_k d\beta_k \right) - \\ &\tilde{C}_{55}^k \frac{1}{R_{\alpha}^k} J_{\alpha}^k \int_{\Omega^k} (\psi_{\alpha_i} \psi_{\beta_j}) d\alpha_k d\beta_k \\ &+ \tilde{C}_{55}^k \frac{1}{(R_{\alpha}^k)^2} J_{\frac{\beta}{\alpha}}^k \int_{\Omega^k} (\psi_{\alpha_i} \psi_{\beta_j}) d\alpha_k d\beta_k \Big) \end{aligned}$$

$$\begin{aligned} K_{u_x u_y}^{\tau_{u_x} s_{u_y}} &= \tilde{C}_{16}^k J_{\frac{\beta}{\alpha}}^k \int_{\Omega^k} (\psi_{\alpha_i, \alpha} \psi_{\beta_j, \alpha}) d\alpha_k d\beta_k \\ &+ \tilde{C}_{12}^k J^k \int_{\Omega^k} (\psi_{\alpha_i, \alpha} \psi_{\beta_j, \beta}) d\alpha_k d\beta_k + \\ &\tilde{C}_{66}^k J^k \int_{\Omega^k} (\psi_{\alpha_i, \beta} \psi_{\beta_j, \alpha}) d\alpha_k d\beta_k \\ &+ \tilde{C}_{26}^k J_{\frac{\beta}{\alpha}}^k \int_{\Omega^k} (\psi_{\alpha_i, \beta} \psi_{\beta_j, \beta}) d\alpha_k d\beta_k \\ &+ \tilde{C}_{45}^k J_{\alpha \beta}^k \int_{\Omega^k} (\psi_{\alpha_i} \psi_{\beta_j}) d\alpha_k d\beta_k \\ &+ \delta_D \times \left( -\tilde{C}_{45}^k \frac{1}{R_{\beta}^k} J_{\alpha}^k \int_{\Omega^k} (\psi_{\alpha_i} \psi_{\beta_j}) d\alpha_k d\beta_k \right) - \\ &\tilde{C}_{45}^k \frac{1}{R_{\alpha}^k} J_{\beta}^k \int_{\Omega^k} (\psi_{\alpha_i} \psi_{\beta_j}) d\alpha_k d\beta_k \\ &+ \tilde{C}_{45}^k \frac{1}{R_{\alpha}^k R_{\beta}^k} J^k \int_{\Omega^k} (\psi_{\alpha_i} \psi_{\beta_j}) d\alpha_k d\beta_k \Big) \end{aligned}$$

$$\begin{aligned} K_{u_x u_z}^{\tau_{u_x} s_{u_z}} &= \tilde{C}_{13}^k J_{\beta}^k \int_{\Omega^k} (\psi_{\alpha_i, \alpha} \psi_{\beta_j}) d\alpha_k d\beta_k \\ &+ \tilde{C}_{55}^k J_{\beta}^k \int_{\Omega^k} (\psi_{\alpha_i} \psi_{\beta_j, \alpha}) d\alpha_k d\beta_k \\ &\tilde{C}_{11}^k \frac{1}{R_{\alpha}^k} J_{\frac{\beta}{\alpha}}^k \int_{\Omega^k} (\psi_{\alpha_i, \alpha} \psi_{\beta_j}) d\alpha_k d\beta_k \\ &+ \tilde{C}_{12}^k \frac{1}{R_{\beta}^k} J^k \int_{\Omega^k} (\psi_{\alpha_i, \alpha} \psi_{\beta_j}) d\alpha_k d\beta_k \\ &+ \tilde{C}_{16}^k \frac{1}{R_{\alpha}^k} J^k \int_{\Omega^k} (\psi_{\alpha_i, \beta} \psi_{\beta_j}) d\alpha_k d\beta_k \\ &+ \tilde{C}_{26}^k \frac{1}{R_{\beta}^k} J_{\frac{\beta}{\alpha}}^k \int_{\Omega^k} (\psi_{\alpha_i, \beta} \psi_{\beta_j}) d\alpha_k d\beta_k - \\ &\delta_D \times \left( \tilde{C}_{55}^k \frac{1}{R_{\alpha}^k} J_{\frac{\beta}{\alpha}}^k \int_{\Omega^k} (\psi_{\alpha_i} \psi_{\beta_j, \alpha}) d\alpha_k d\beta_k \right) \\ &+ \tilde{C}_{45}^k \frac{1}{R_{\alpha}^k} J^k \int_{\Omega^k} (\psi_{\alpha_i} \psi_{\beta_j, \beta}) d\alpha_k d\beta_k \Big) \end{aligned}$$



$$\begin{aligned}
& + \tilde{C}_{13}^k \frac{1}{R_z^k} J_\beta^k \tau_{u_z} s_{u_z} \left[ \int_{\Omega^k} (\psi_{\alpha_i} \psi_{\alpha_j}) d\alpha_k d\beta_k \right] \\
& + \tilde{C}_{23}^k \frac{1}{R_\beta^k} J_\alpha^k \tau_{u_z} s_{u_z} \left[ \int_{\Omega^k} (\psi_{\alpha_i} \psi_{\alpha_j}) d\alpha_k d\beta_k \right] \\
& + \tilde{C}_{11}^k \frac{1}{(R_z^k)^2} J_\beta^k \tau_{u_z} s_{u_z} \left[ \int_{\Omega^k} (\psi_{\alpha_i} \psi_{\alpha_j}) d\alpha_k d\beta_k \right] \\
& + \tilde{C}_{12}^k \frac{1}{(R_z^k R_\beta^k)} J_\beta^k \tau_{u_z} s_{u_z} \left[ \int_{\Omega^k} (\psi_{\alpha_i} \psi_{\alpha_j}) d\alpha_k d\beta_k \right] \\
& + \tilde{C}_{12}^k \frac{1}{(R_z^k R_\beta^k)} J_\alpha^k \tau_{u_z} s_{u_z} \left[ \int_{\Omega^k} (\psi_{\alpha_i} \psi_{\alpha_j}) d\alpha_k d\beta_k \right] \\
& + \tilde{C}_{22}^k \frac{1}{(R_\beta^k)^2} J_\alpha^k \tau_{u_z} s_{u_z} \left[ \int_{\Omega^k} (\psi_{\alpha_i} \psi_{\alpha_j}) d\alpha_k d\beta_k \right]
\end{aligned}$$

$$\begin{aligned}
M_{u_z u_z}^{\tau_{u_z} s_{u_z}} &= \rho^k J^k \tau_{u_z} s_{u_z} \left[ \int_{\Omega^k} (\psi_{\alpha_i} \psi_{\alpha_j}) d\alpha_k d\beta_k \right] \\
M_{u_\beta u_\beta}^{\tau_{u_\beta} s_{u_\beta}} &= \rho^k J^k \tau_{u_\beta} s_{u_\beta} \left[ \int_{\Omega^k} (\psi_{\beta_i} \psi_{\beta_j}) d\alpha_k d\beta_k \right] \\
M_{u_z u_z}^{\tau_{u_z} s_{u_z}} &= \rho^k J^k \tau_{u_z} s_{u_z} \left[ \int_{\Omega^k} (\psi_{z_i} \psi_{z_j}) d\alpha_k d\beta_k \right] \quad (31)
\end{aligned}$$

By exploiting the use of the relations  $\delta T^k = -\delta L_{int}^k$  and  $\delta U^k = \delta L_{int}^k$  (see [30]), the PVD in Eq. (22) for further details can be rewritten as:

$$\delta(T^k - U^k) = 0 \quad (32)$$

which represents a minimization of the total energy of the system with respect to the introduced degrees of freedom [30,64], therefore it can be equivalently written as:

$$\begin{aligned}
\frac{\partial(T^k - U^k)}{\partial U_{\alpha\tau_{u_z} i}^k} &= 0 \quad \text{with } i = 1, \dots, \mathcal{N}; \quad \tau_{u_z} = b_{u_z}, r_{u_z}, t_{u_z} \quad r_{u_z} = 2, 3, \dots, N_{u_z} - 1 \\
\frac{\partial(T^k - U^k)}{\partial U_{\beta\tau_{u_\beta} i}^k} &= 0 \quad \text{with } i = 1, \dots, \mathcal{N}; \quad \tau_{u_\beta} = b_{u_\beta}, r_{u_\beta}, t_{u_\beta} \quad r_{u_\beta} = 2, 3, \dots, N_{u_\beta} - 1 \\
\frac{\partial(T^k - U^k)}{\partial U_{z\tau_{u_z} i}^k} &= 0 \quad \text{with } i = 1, \dots, \mathcal{N}; \quad \tau_{u_z} = b_{u_z}, b_{u_z}, t_{u_z} \quad r_{u_z} = 2, 3, \dots, N_{u_z} - 1
\end{aligned} \quad (33)$$

The Ritz method leads to the discrete form of the governing differential equations in terms of the Ritz primary fundamental nuclei:

$$\delta \mathbf{U}_{ci}^{kT} : \left[ \mathbf{K}^{ktsij} - \omega_{ij}^2 \mathbf{M}^{ktsij} \right] \mathbf{U}_{sj}^k = 0 \quad (34)$$

The free-vibration response of the multilayered shells leads to the following eigenvalues problem:

$$\| \mathbf{K}^{ktsij} - \omega_{ij}^2 \mathbf{M}^{ktsij} \| = 0 \quad (35)$$

The double bars denote the determinant. Each Ritz fundamental secondary nucleus of the CUF has to be expanded individually according to the expansion order chosen for the displacement components [30]. When the expansions have been performed then they can be arranged as in Eq. (36) and generate the Ritz fundamental primary nuclei related at the particular theory used.

$$\mathbf{K}^{ktsij} = \begin{bmatrix} \mathbf{K}_{u_z u_z} & \mathbf{K}_{u_z u_\beta} & \mathbf{K}_{u_z u_z} \\ \mathbf{K}_{u_\beta u_z} & \mathbf{K}_{u_\beta u_\beta} & \mathbf{K}_{u_\beta u_z} \\ \mathbf{K}_{u_z u_z} & \mathbf{K}_{u_z u_\beta} & \mathbf{K}_{u_z u_z} \end{bmatrix} \quad \mathbf{M}^{ktsij} = \begin{bmatrix} \mathbf{M}_{u_z u_z} & 0 & 0 \\ 0 & \mathbf{M}_{u_\beta u_\beta} & 0 \\ 0 & 0 & \mathbf{M}_{u_z u_z} \end{bmatrix} \quad (36)$$

## 6. Governing differential equations of doubly-curved shells

In order to derive the governing differential equations and natural boundary conditions the Gauss theorem is applied:

$$\begin{aligned}
\int_{\Omega_k} ((\mathbf{D}_p) \delta \mathbf{a}^k)^T \mathbf{a}^k d\Omega_k &= - \int_{\Omega_k} \delta \mathbf{a}^k ((\mathbf{D}_p)^T \delta \mathbf{a}^k) d\Omega_k + \int_{\Gamma^k} \delta \mathbf{a}^k ((\mathbf{I}_p)^T \delta \mathbf{a}^k) d\Gamma^k \\
\int_{\Omega_k} ((\mathbf{D}_\Omega) \delta \mathbf{a}^k)^T \mathbf{a}^k d\Omega_k &= - \int_{\Omega_k} \delta \mathbf{a}^k ((\mathbf{D}_\Omega)^T \delta \mathbf{a}^k) d\Omega_k + \int_{\Gamma^k} \delta \mathbf{a}^k ((\mathbf{I}_\Omega)^T \delta \mathbf{a}^k) d\Gamma^k
\end{aligned} \quad (37)$$

where  $\mathbf{a}$  can be displacement or stress variables and the introduced  $\mathbf{I}_p$  and  $\mathbf{I}_\Omega$  arrays are:

$$\mathbf{I}_p = \begin{bmatrix} \frac{n_z}{H_z^k} & 0 & 0 \\ 0 & \frac{n_\beta}{H_\beta^k} & 0 \\ \frac{n_\beta}{H_\beta^k} & \frac{n_z}{H_z^k} & 0 \end{bmatrix}, \quad \mathbf{I}_\Omega = \begin{bmatrix} 0 & 0 & \frac{n_z}{H_z^k} \\ 0 & 0 & \frac{n_\beta}{H_\beta^k} \\ 0 & 0 & 0 \end{bmatrix} \quad (38)$$

The normal to the boundary of domain  $\Omega_k$  is:

$$\hat{\mathbf{n}} = \begin{bmatrix} n_\alpha \\ n_\beta \end{bmatrix} = \begin{bmatrix} \cos(\varphi_\alpha) \\ \cos(\varphi_\beta) \end{bmatrix} \quad (39)$$

where  $\varphi_\alpha$  and  $\varphi_\beta$  are the direction cosines, namely, the angles between the normal  $\hat{\mathbf{n}}$  and the directions  $\alpha$  and  $\beta$ , respectively. The governing differential equations and natural boundary conditions (Neumann-type) on  $\Gamma^k$ , for a doubly-curved anisotropic composite shell at multilayer level can be written as:

$$\begin{aligned}
\sum_{k=1}^{N_l} \int_{\Omega_k} \int_{A^k} \delta \mathbf{u}_\tau \left( - [(\mathbf{F}_\tau)^T (\mathbf{D}_p)^T + (\mathbf{F}_\tau)^T (\mathbf{A}_p)^T] [\tilde{\mathbf{C}}_{pp}^k \mathbf{D}_p(\mathbf{F}_\tau) + \tilde{\mathbf{C}}_{pp}^k \mathbf{A}_p(\mathbf{F}_\tau) \right. \\
+ \tilde{\mathbf{C}}_{pn}^k \mathbf{D}_{np}(\mathbf{F}_\tau) + \tilde{\mathbf{C}}_{pn}^k \delta_D \tilde{\mathbf{A}}_n^k \mathbf{D}_{np}(\mathbf{F}_\tau) + \tilde{\mathbf{C}}_{pn}^k \mathbf{D}_{nz}(\mathbf{F}_\tau) - [(\mathbf{F}_\tau)^T (\mathbf{D}_{np})^T \\
+ (\mathbf{F}_\tau)^T (\delta_D \mathbf{A}_n)^T + (\mathbf{F}_\tau)^T (\mathbf{D}_{nz})^T] + [\tilde{\mathbf{C}}_{np}^k \mathbf{D}_p(\mathbf{F}_\tau) + \tilde{\mathbf{C}}_{np}^k \mathbf{A}_p(\mathbf{F}_\tau) \\
+ \tilde{\mathbf{C}}_{nn}^k \mathbf{D}_{np}(\mathbf{F}_\tau) + \tilde{\mathbf{C}}_{nn}^k \delta_D \tilde{\mathbf{A}}_n^k \mathbf{D}_{np}(\mathbf{F}_\tau) + \tilde{\mathbf{C}}_{nn}^k \mathbf{D}_{nz}(\mathbf{F}_\tau)] \Big) \mathbf{u}_s d\Omega_k dz + \\
\sum_{k=1}^{N_l} \int_{\Omega_k} \int_{A^k} \delta \mathbf{u}_\tau \left( (\mathbf{F}_\tau)^T (\mathbf{I}_p)^T [\tilde{\mathbf{C}}_{pp}^k \mathbf{D}_p(\mathbf{F}_\tau) + \tilde{\mathbf{C}}_{pp}^k \mathbf{A}_p(\mathbf{F}_\tau) + \tilde{\mathbf{C}}_{pn}^k \mathbf{D}_{np}(\mathbf{F}_\tau) \right. \\
+ \tilde{\mathbf{C}}_{pn}^k \delta_D \mathbf{A}_n(\mathbf{F}_\tau) + \tilde{\mathbf{C}}_{pn}^k \mathbf{D}_{nz}(\mathbf{F}_\tau) + (\mathbf{F}_\tau)^T (\mathbf{I}_{np})^T [\tilde{\mathbf{C}}_{np}^k \mathbf{D}_p(\mathbf{F}_\tau) + \tilde{\mathbf{C}}_{np}^k \mathbf{A}_p(\mathbf{F}_\tau) \\
+ \tilde{\mathbf{C}}_{nn}^k \mathbf{D}_{np}(\mathbf{F}_\tau) + \tilde{\mathbf{C}}_{nn}^k \delta_D \mathbf{A}_n(\mathbf{F}_\tau) + \tilde{\mathbf{C}}_{nn}^k \mathbf{D}_{nz}(\mathbf{F}_\tau)] \Big) \mathbf{u}_s d\Omega_k dz \\
= \sum_{k=1}^{N_l} \int_{\Omega_k} \int_{A^k} \delta \mathbf{u}_\tau \left( \rho^k (\mathbf{F}_\tau)^T (\mathbf{F}_s) \right) \ddot{\mathbf{u}}_s d\Omega_k dz \quad (40)
\end{aligned}$$

and in compact form are:

$$\begin{aligned}
\delta \mathbf{u}_\tau : \quad \mathbf{K}_{uu}^{kts} \mathbf{u}_s + \mathbf{M}_{uu}^{kts} \ddot{\mathbf{u}}_s &= 0 \\
\Gamma_k^m : \quad \mathbf{\Pi}_{uu}^{kts} \mathbf{u}_s = \mathbf{\Pi}_{uu}^{kts} \bar{\mathbf{u}}_s \quad \Gamma_k^g : \quad \mathbf{u}_s = \bar{\mathbf{u}}_s
\end{aligned} \quad (41)$$

where

$$\begin{aligned}
\mathbf{K}_{uu}^{kts} &= \int_{A^k} \left( - [(\mathbf{F}_\tau)^T (\mathbf{D}_p)^T + (\mathbf{F}_\tau)^T (\mathbf{A}_p)^T] [\tilde{\mathbf{C}}_{pp}^k \mathbf{D}_p(\mathbf{F}_\tau) + \tilde{\mathbf{C}}_{pp}^k \mathbf{A}_p(\mathbf{F}_\tau) \right. \\
&+ \tilde{\mathbf{C}}_{pn}^k \mathbf{D}_{np}(\mathbf{F}_\tau) + \tilde{\mathbf{C}}_{pn}^k \delta_D \tilde{\mathbf{A}}_n^k \mathbf{D}_{np}(\mathbf{F}_\tau) + \tilde{\mathbf{C}}_{pn}^k \mathbf{D}_{nz}(\mathbf{F}_\tau) - [(\mathbf{F}_\tau)^T (\mathbf{D}_{np})^T \\
&+ (\mathbf{F}_\tau)^T (\delta_D \mathbf{A}_n)^T + (\mathbf{F}_\tau)^T (\mathbf{D}_{nz})^T] + [\tilde{\mathbf{C}}_{np}^k \mathbf{D}_p(\mathbf{F}_\tau) + \tilde{\mathbf{C}}_{np}^k \mathbf{A}_p(\mathbf{F}_\tau) \\
&+ \tilde{\mathbf{C}}_{nn}^k \mathbf{D}_{np}(\mathbf{F}_\tau) + \tilde{\mathbf{C}}_{nn}^k \delta_D \tilde{\mathbf{A}}_n^k \mathbf{D}_{np}(\mathbf{F}_\tau) + \tilde{\mathbf{C}}_{nn}^k \mathbf{D}_{nz}(\mathbf{F}_\tau)] \Big) H_\alpha^k H_\beta^k dz \\
\mathbf{\Pi}_{uu}^{kts} &= \int_{A^k} \left( (\mathbf{F}_\tau)^T (\mathbf{I}_p)^T [\tilde{\mathbf{C}}_{pp}^k \mathbf{D}_p(\mathbf{F}_\tau) + \tilde{\mathbf{C}}_{pp}^k \mathbf{A}_p(\mathbf{F}_\tau) + \tilde{\mathbf{C}}_{pn}^k \mathbf{D}_{np}(\mathbf{F}_\tau) \right. \\
&+ \tilde{\mathbf{C}}_{pn}^k \delta_D \mathbf{A}_n(\mathbf{F}_\tau) + \tilde{\mathbf{C}}_{pn}^k \mathbf{D}_{nz}(\mathbf{F}_\tau) + (\mathbf{F}_\tau)^T (\mathbf{I}_{np})^T [\tilde{\mathbf{C}}_{np}^k \mathbf{D}_p(\mathbf{F}_\tau) \\
&+ \tilde{\mathbf{C}}_{np}^k \mathbf{A}_p(\mathbf{F}_\tau) + \tilde{\mathbf{C}}_{nn}^k \mathbf{D}_{np}(\mathbf{F}_\tau) + \tilde{\mathbf{C}}_{nn}^k \delta_D \mathbf{A}_n(\mathbf{F}_\tau) + \tilde{\mathbf{C}}_{nn}^k \mathbf{D}_{nz}(\mathbf{F}_\tau)] \Big) H_\alpha^k H_\beta^k dz \\
\mathbf{M}_{uu}^{kts} &= \int_{A^k} \rho^k (\mathbf{F}_\tau)^T (\mathbf{F}_s) H_\alpha^k H_\beta^k dz \quad (42)
\end{aligned}$$





$$\begin{aligned} \Pi_{uu}^{k \tau_{u\beta} S_{uz}} &= n_\alpha \tilde{C}_{16}^k J_{\frac{\beta}{\alpha}}^{k \tau_{u\beta} S_{uz}} \left( \frac{\partial}{\partial \alpha} \right)_{S_{uz}} + n_\beta \tilde{C}_{26}^k J_{\frac{\alpha}{\beta}}^{k \tau_{u\beta} S_{uz}} \left( \frac{\partial}{\partial \beta} \right)_{S_{uz}} \\ &+ n_\beta \tilde{C}_{12}^k J_{\frac{\alpha}{\beta}}^{k \tau_{u\beta} S_{uz}} \left( \frac{\partial}{\partial \alpha} \right)_{S_{uz}} + n_\alpha \tilde{C}_{66}^k J_{\frac{\alpha}{\beta}}^{k \tau_{u\beta} S_{uz}} \left( \frac{\partial}{\partial \beta} \right)_{S_{uz}} \end{aligned}$$

$$\begin{aligned} \Pi_{uu}^{k \tau_{u\beta} S_{u\beta}} &= n_\alpha \tilde{C}_{66}^k J_{\frac{\beta}{\alpha}}^{k \tau_{u\beta} S_{u\beta}} \left( \frac{\partial}{\partial \alpha} \right)_{S_{u\beta}} + n_\beta \tilde{C}_{22}^k J_{\frac{\alpha}{\beta}}^{k \tau_{u\beta} S_{u\beta}} \left( \frac{\partial}{\partial \beta} \right)_{S_{u\beta}} \\ &+ n_\beta \tilde{C}_{26}^k J_{\frac{\alpha}{\beta}}^{k \tau_{u\beta} S_{u\beta}} \left( \frac{\partial}{\partial \alpha} \right)_{S_{u\beta}} + n_\alpha \tilde{C}_{26}^k J_{\frac{\alpha}{\beta}}^{k \tau_{u\beta} S_{u\beta}} \left( \frac{\partial}{\partial \beta} \right)_{S_{u\beta}} \end{aligned}$$

$$\begin{aligned} \Pi_{uu}^{k \tau_{u\beta} S_{uz}} &= n_\alpha \frac{1}{R_{\alpha k}} \tilde{C}_{16}^k J_{\frac{\beta}{\alpha}}^{k \tau_{u\beta} S_{uz}} + n_\alpha \frac{1}{R_{\beta k}} \tilde{C}_{26}^k J_{\frac{\alpha}{\beta}}^{k \tau_{u\beta} S_{uz}} + n_\alpha \tilde{C}_{36}^k J_{\frac{\alpha}{\beta}}^{k \tau_{u\beta} S_{uz}} + n_\beta \\ &\times \frac{1}{R_{\alpha k}} \tilde{C}_{12}^k J_{\frac{\alpha}{\beta}}^{k \tau_{u\beta} S_{uz}} + n_\beta \frac{1}{R_{\beta k}} \tilde{C}_{22}^k J_{\frac{\alpha}{\beta}}^{k \tau_{u\beta} S_{uz}} + n_\beta \tilde{C}_{23}^k J_{\frac{\alpha}{\beta}}^{k \tau_{u\beta} S_{uz}} \end{aligned}$$

$$\begin{aligned} \Pi_{uu}^{k \tau_{uz} S_{uz}} &= -n_\alpha \frac{1}{R_{\alpha k}} \tilde{C}_{55}^k J_{\frac{\beta}{\alpha}}^{k \tau_{uz} S_{uz}} + n_\alpha \tilde{C}_{55}^k J_{\frac{\beta}{\alpha}}^{k \tau_{uz} S_{uz}} - n_\beta \frac{1}{R_{\alpha k}} \tilde{C}_{45}^k J_{\frac{\alpha}{\beta}}^{k \tau_{uz} S_{uz}} \\ &+ n_\beta \tilde{C}_{45}^k J_{\frac{\alpha}{\beta}}^{k \tau_{uz} S_{uz}} \end{aligned}$$

$$\begin{aligned} \Pi_{uu}^{k \tau_{uz} S_{u\beta}} &= -n_\alpha \frac{1}{R_{\beta k}} \tilde{C}_{45}^k J_{\frac{\alpha}{\beta}}^{k \tau_{uz} S_{u\beta}} + n_\alpha \tilde{C}_{45}^k J_{\frac{\alpha}{\beta}}^{k \tau_{uz} S_{u\beta}} - n_\beta \frac{1}{R_{\beta k}} \tilde{C}_{44}^k J_{\frac{\alpha}{\beta}}^{k \tau_{uz} S_{u\beta}} \\ &+ n_\beta \tilde{C}_{44}^k J_{\frac{\alpha}{\beta}}^{k \tau_{uz} S_{u\beta}} \end{aligned}$$

$$\begin{aligned} \Pi_{uu}^{k \tau_{uz} S_{uz}} &= n_\alpha \tilde{C}_{55}^k J_{\frac{\beta}{\alpha}}^{k \tau_{uz} S_{uz}} \left( \frac{\partial}{\partial \alpha} \right)_{S_{uz}} + n_\beta \tilde{C}_{44}^k J_{\frac{\alpha}{\beta}}^{k \tau_{uz} S_{uz}} \left( \frac{\partial}{\partial \beta} \right)_{S_{uz}} \\ &+ n_\beta \tilde{C}_{45}^k J_{\frac{\alpha}{\beta}}^{k \tau_{uz} S_{uz}} \left( \frac{\partial}{\partial \alpha} \right)_{S_{uz}} + n_\alpha \tilde{C}_{45}^k J_{\frac{\alpha}{\beta}}^{k \tau_{uz} S_{uz}} \left( \frac{\partial}{\partial \beta} \right)_{S_{uz}} \end{aligned} \tag{44}$$

Finally the fundamental primary mass nucleus  $\mathbf{M}_{uu}$  components can be written as:

$$\begin{aligned} \mathbf{M}_{uu}^{k \tau_{uz} S_{uz}} &= \rho^k J^{k \tau_{uz} S_{uz}} \quad \mathbf{M}_{uu}^{k \tau_{uz} S_{u\beta}} = 0 \quad \mathbf{M}_{uu}^{k \tau_{uz} S_{uz}} = 0 \\ \mathbf{M}_{uu}^{k \tau_{u\beta} S_{uz}} &= 0 \quad \mathbf{M}_{uu}^{k \tau_{u\beta} S_{u\beta}} = \rho^k J^{k \tau_{u\beta} S_{u\beta}} \quad \mathbf{M}_{uu}^{k \tau_{u\beta} S_{uz}} = 0 \\ \mathbf{M}_{uu}^{k \tau_{uz} S_{uz}} &= 0 \quad \mathbf{M}_{uu}^{k \tau_{uz} S_{u\beta}} = 0 \quad \mathbf{M}_{uu}^{k \tau_{uz} S_{uz}} = \rho^k J^{k \tau_{uz} S_{uz}} \end{aligned} \tag{45}$$

**7. Numerical results and discussion**

Numerical results have been computed taking into account cross-ply and angle-ply simply supported square shells, materials in Table 2 and a set of trigonometric trial functions following defined:

$$\begin{aligned} \psi_{\alpha mn}(\alpha, \beta) &= \sum_{m,n} \cos\left(\frac{m\pi\alpha}{a}\right) \sin\left(\frac{n\pi\beta}{b}\right) \\ \psi_{\beta mn}(\alpha, \beta) &= \sum_{m,n} \sin\left(\frac{m\pi\alpha}{a}\right) \cos\left(\frac{n\pi\beta}{b}\right) \\ \psi_{z mn}(\alpha, \beta) &= \sum_{m,n} \sin\left(\frac{m\pi\alpha}{a}\right) \sin\left(\frac{n\pi\beta}{b}\right) \end{aligned} \tag{46}$$

**Table 1**  
List of acronyms used in tables to denote the shell theories.

Acronym	Description
<i>Cross-ply hollow circular cylindrical shells</i>	
3D exact	3D exact elasticity solution by Ye and Soldatos, [88]
PAR <sub>ds</sub>	Discontinuous interlaminar stresses distributed parabolically by Timarci and Soldatos, [89]
HYT <sub>ds</sub>	Discontinuous interlaminar stresses distributed hyperbolically by Timarci and Soldatos, [89]
UNI <sub>cs</sub>	Continuous interlaminar stresses distributed uniformly by Timarci and Soldatos, [55]
PAR <sub>cs</sub>	Continuous interlaminar stresses distributed parabolically by Timarci and Soldatos, [89]
HYT <sub>cs</sub>	Continuous interlaminar stresses distributed hyperbolically by Timarci and Soldatos, [89]
ZZD	Refined zig-zag theory by Di Sciuva and Carrera, [90]
HSDTM	Refined higher Order theory by Matsunaga, [91]
<i>Cross-ply shallow cylindrical and spherical shells</i>	
WLC	Wavelet collocation by Ferreira, [59]
RBF	Radial basis functions by Ferreira, [92]
SRBC	Sinusoidal radial basis collocation by Ferreira, [93]
LWRBC	Layer-wise radial basis collocation by Ferreira, [60]
<i>Cross-ply deep cylindrical shells</i>	
FSDTQ	First order shear deformation theory by Qatu, [58]
3D FEM	3D FEM solution by Qatu, [58]
<i>Angle-ply shallow cylindrical and spherical shells</i>	
R-FSDT	Ritz method using algebraic polynomials by Qatu, [94]
<i>Angle-ply deep cylindrical shells</i>	
R-FSDT	Ritz method using algebraic polynomials by Qatu, [94]

**Table 2**  
Materials.

Mat-1		Mat-2 E-glass/epoxy (E/E)	
E <sub>1</sub> /E <sub>2</sub>	E <sub>3</sub> /E <sub>2</sub>	G <sub>12</sub> /E <sub>2</sub> , G <sub>13</sub> /E <sub>2</sub>	G <sub>23</sub> /E <sub>2</sub>
25	1	0.5	0.2
E <sub>1</sub> [GPa]	E <sub>2</sub> , E <sub>3</sub> [GPa]	G <sub>12</sub> , G <sub>13</sub> [GPa]	G <sub>23</sub> [GPa]
60.7	24.8	12	12

v <sub>12</sub> , v <sub>13</sub>	v <sub>23</sub>	v <sub>12</sub> , v <sub>13</sub>	v <sub>23</sub>
0.25	0.25	0.23	0.23

**Table 3**

Dimensionless fundamental circular frequency parameter  $\hat{\omega} = \omega a^2 \sqrt{\frac{\rho}{E_2}}$ , of square circular cylindrical shells with staking sequence  $[0^\circ/90^\circ/90^\circ/0^\circ]$ ,  $m = 1, n$  in brackets, length-to-thickness ratio  $a/h = 10$ , ED shell models and varying the radius-to-length ratios.

Theory	5	10	20	50	100	Ave. err. (%)	Max err. (%)
<i>R<sub>β</sub>/a</i>							
3D exact	10.305 (14)	10.027 (22)	9.902 (30)	9.834 (24)	9.815 (1)		
PAR <sub>ds</sub>	10.496	10.223	10.099	10.032	10.013	(1.97)	(2.02)
HYT <sub>ds</sub>	10.496	10.226	10.103	10.036	10.018	(2.00)	(2.07)
UNI <sub>cs</sub>	10.462	10.187	10.063	9.996	9.977	(1.61)	(1.65)
PAR <sub>cs</sub>	10.329	10.051	9.927	9.859	9.840	(0.25)	(0.25)
HYT <sub>cs</sub>	10.328	10.050	9.925	9.858	9.839	(0.23)	(0.24)
ZZD	10.462	10.187	10.063	9.996	9.971	(1.60)	(1.65)
HSDTM	10.3661	10.0893	9.9652	9.8976	9.8789	(0.63)	(0.65)
<i>Present ED models C-E<sup>a</sup></i>							
ED <sub>111</sub>	11.3183 (14) <sup>c</sup>	11.0645 (22)	10.9461 (30)	10.8795 (24)	10.8619 (1)	(10.40)	(10.67)
ED <sub>222</sub>	11.2915	11.0403	10.9246	10.8601	10.8427	(10.18)	(10.47)
ED <sub>333</sub>	10.4533	10.1786	10.0552	9.98777	9.96914	(1.53)	(1.57)
ED <sub>444</sub>	10.4528	10.1782	10.0549	9.98743	9.96880	(1.52)	(1.57)
ED <sub>555</sub>	10.3843	10.1079	9.98408	9.91658	9.89787	(0.82)	(0.84)
ED <sub>666</sub>	10.3842	10.1079	9.98407	9.91657	9.89786	(0.82)	(0.84)
ED <sub>777</sub>	10.3835	10.1072	9.98345	9.91596	9.89725	(0.81)	(0.84)
ED <sub>888</sub>	10.3835	10.1072	9.98344	9.91596	9.89725	(0.81)	(0.84)
<i>Present ED models MD-E<sup>b</sup></i>							
ED <sub>111</sub>	11.3225	11.0654	10.9462	10.8795	10.8619	(10.41)	(10.67)
ED <sub>222</sub>	11.2958	11.0412	10.9247	10.8601	10.8427	(10.19)	(10.47)
ED <sub>333</sub>	10.4578	10.1795	10.0554	9.98777	9.96914	(1.54)	(1.57)
ED <sub>444</sub>	10.4572	10.1791	10.0550	9.98743	9.96880	(1.53)	(1.57)
ED <sub>555</sub>	10.3887	10.1088	9.98424	9.91658	9.89787	(0.83)	(0.84)
ED <sub>666</sub>	10.3887	10.1088	9.98422	9.91657	9.89786	(0.83)	(0.84)
ED <sub>777</sub>	10.3880	10.1081	9.98360	9.91596	9.89725	(0.82)	(0.84)
ED <sub>888</sub>	10.3880	10.1081	9.98359	9.91596	9.89725	(0.82)	(0.84)

<sup>a</sup> C-E (Complete equations).

<sup>b</sup> DM-E (Donnell–Mushtari’s shallow shell-type equations).

<sup>c</sup> The half-wave number  $n$  is the same for all the higher order models and for the C-E and DM-E.

**Table 4**

Dimensionless fundamental circular frequency parameter  $\hat{\omega} = \omega a^2 \sqrt{\frac{\rho}{E_2}}$ , of square circular cylindrical shells with staking sequence  $[0^\circ/90^\circ/90^\circ/0^\circ]$ ,  $m = 1, n$  in brackets, length-to-thickness ratio  $a/h = 10$ , EDZ shell models and varying the radius-to-length ratios.

Theory	5	10	20	50	100	Ave. err. (%)	Max err. (%)
<i>R<sub>β</sub>/a</i>							
3D exact	10.305 (14)	10.027 (22)	9.902 (30)	9.834 (24)	9.815 (1)		
PAR <sub>ds</sub>	10.496	10.223	10.099	10.032	10.013	(1.97)	(2.02)
HYT <sub>ds</sub>	10.496	10.226	10.103	10.036	10.018	(2.00)	(2.07)
UNI <sub>cs</sub>	10.462	10.187	10.063	9.996	9.977	(1.61)	(1.65)
PAR <sub>cs</sub>	10.329	10.051	9.927	9.859	9.840	(0.25)	(0.25)
HYT <sub>cs</sub>	10.328	10.050	9.925	9.858	9.839	(0.23)	(0.24)
ZZD	10.462	10.187	10.063	9.996	9.971	(1.60)	(1.65)
HSDTM	10.3661	10.0893	9.9652	9.8976	9.8789	(0.63)	(0.65)
<i>Present EDZ models C-E<sup>a</sup></i>							
EDZ <sub>111</sub>	11.3133 (14) <sup>c</sup>	11.0599 (22)	10.9419 (30)	10.8756 (24)	10.8581 (1)	(10.36)	(10.63)
EDZ <sub>222</sub>	11.2914	11.0403	10.9246	10.8601	10.8427	(10.18)	(10.47)
EDZ <sub>333</sub>	10.4532	10.1785	10.0551	9.98766	9.96903	(1.53)	(1.57)
EDZ <sub>444</sub>	10.4527	10.1782	10.0548	9.98742	9.96880	(1.52)	(1.57)
EDZ <sub>555</sub>	10.3842	10.1079	9.98406	9.91656	9.89785	(0.82)	(0.84)
EDZ <sub>666</sub>	10.3842	10.1079	9.98406	9.91656	9.89785	(0.82)	(0.84)
EDZ <sub>777</sub>	10.3835	10.1072	9.98344	9.91595	9.89724	(0.81)	(0.84)
EDZ <sub>888</sub>	10.3835	10.1072	9.98344	9.91595	9.89724	(0.81)	(0.84)
<i>Present EDZ models MD-E<sup>b</sup></i>							
EDZ <sub>111</sub>	11.3175	11.0607	10.9420	10.8757	10.8581	(10.37)	(10.63)
EDZ <sub>222</sub>	11.2957	11.0412	10.9247	10.8601	10.8427	(10.19)	(10.47)
EDZ <sub>333</sub>	10.4576	10.1794	10.0553	9.98766	9.96903	(1.54)	(1.57)
EDZ <sub>444</sub>	10.4571	10.1791	10.0550	9.98743	9.96880	(1.53)	(1.57)
EDZ <sub>555</sub>	10.3886	10.1088	9.98421	9.91657	9.89785	(0.83)	(0.84)
EDZ <sub>666</sub>	10.3886	10.1088	9.98422	9.91657	9.89785	(0.83)	(0.84)
EDZ <sub>777</sub>	10.3880	10.1081	9.98359	9.91596	9.89724	(0.82)	(0.84)
EDZ <sub>888</sub>	10.3880	10.1081	9.98359	9.91596	9.89724	(0.82)	(0.84)

<sup>a</sup> C-E (Complete equations).

<sup>b</sup> DM-E (Donnell–Mushtari’s shallow shell-type equations).

<sup>c</sup> The half-wave number  $n$  is the same for all the higher order models and for the C-E and DM-E.

**Table 5**  
Dimensionless fundamental circular frequency parameter  $\hat{\omega} = \omega a^2 \sqrt{\frac{\rho}{E_2}}$  of square circular cylindrical shells with stacking sequence  $[0^\circ/90^\circ/90^\circ/0^\circ]$ ,  $m = 1$ ,  $n$  in brackets, length-to thickness ratio  $a/h = 10$ , LD shell models and varying the radius-to-length ratios.

Theory	5	10	20	50	100	Ave. err. (%)	Max err. (%)
$R_\beta/a$							
3D exact	10.305 (14)	10.027 (22)	9.902 (30)	9.834 (24)	9.815 (1)		
PAR <sub>ds</sub>	10.496	10.223	10.099	10.032	10.013	(1.97)	(2.02)
HYT <sub>ds</sub>	10.496	10.226	10.103	10.036	10.018	(2.00)	(2.07)
UNI <sub>cs</sub>	10.462	10.187	10.063	9.996	9.977	(1.61)	(1.65)
PAR <sub>cs</sub>	10.329	10.051	9.927	9.859	9.840	(0.25)	(0.25)
HYT <sub>cs</sub>	10.328	10.050	9.925	9.858	9.839	(0.23)	(0.24)
ZZD	10.462	10.187	10.063	9.996	9.971	(1.60)	(1.65)
HSDTM	10.3661	10.0893	9.9652	9.8976	9.8789	(0.63)	(0.65)
<i>Present LD models C-E<sup>a</sup></i>							
LD <sub>111</sub>	10.3698 (14) <sup>c</sup>	10.0904 (22)	9.96628 (30)	9.89860 (24)	9.87985 (1)	(0.65)	(0.66)
LD <sub>222</sub>	10.3065	10.0280	9.90331	9.83543	9.81658	(0.01)	(0.02)
LD <sub>333</sub>	<b>10.305</b>	<b>10.027</b>	<b>9.902</b>	<b>9.834</b>	<b>9.815</b>	(0.00)	(0.00)
LD <sub>444</sub>	<b>10.305</b>	<b>10.027</b>	<b>9.902</b>	<b>9.834</b>	<b>9.815</b>	(0.00)	(0.00)
<i>Present LD models MD-E<sup>b</sup></i>							
LD <sub>111</sub>	10.3720	10.0913	9.96643	9.89861	9.87985	(0.65)	(0.66)
LD <sub>222</sub>	10.3110	10.0289	9.90346	9.83543	9.81658	(0.03)	(0.06)
LD <sub>333</sub>	10.3099	10.0277	<b>9.902</b>	<b>9.834</b>	<b>9.815</b>	(0.01)	(0.05)
LD <sub>444</sub>	10.3099	10.0277	<b>9.902</b>	<b>9.834</b>	<b>9.815</b>	(0.01)	(0.05)

<sup>a</sup> C-E (Complete equations).

<sup>b</sup> DM-E (Donnell–Mushtari’s shallow shell-type equations).

<sup>c</sup> The half-wave number  $n$  is the same for all the higher order models and for the C-E and DM-E.

**Table 6**  
Dimensionless fundamental circular frequency parameter  $\hat{\omega} = \omega a^2 \sqrt{\frac{\rho}{E_2}}$  of square cross-ply shallow cylindrical shells with stacking sequence  $[0^\circ/90^\circ/0^\circ]$ .

Theory	10					100				
	5	10	20	50	100	5	10	20	50	100
$R_\beta/a$										
WLC	12.2143	12.1758	12.1661	12.1634	12.1629	20.3372	16.6279	15.5590	15.2460	15.2008
RBF	11.8513	11.8076	11.7966	11.7935	11.7930	20.5357	16.6417	15.5106	15.1789	15.1306
SRBC	11.9230	11.9146	11.9125	11.9119	11.9118	20.4656	16.8441	15.7993	15.4938	15.4497
LWRBC	11.8732	11.7073	–	–	11.6516	20.3544	16.6831	–	–	15.2736
<i>Present models C-E<sup>a</sup></i>										
LD <sub>555</sub>	11.5078	11.6376	11.4605	11.4579	11.4575	20.3195	16.6084	15.5390	15.2258	15.1805
LD <sub>111</sub>	11.6295	11.5924	11.5830	11.5804	11.5800	20.3294	16.6204	15.5518	15.2389	15.1937
EDZ <sub>888</sub>	11.5090	11.4707	11.4611	11.4584	11.4580	20.3198	16.6085	15.5390	15.2258	15.1805
EDZ <sub>333</sub>	11.5119	11.4734	11.4638	11.4611	11.4607	20.3200	16.6085	15.5390	15.2258	15.1805
ED <sub>999</sub>	11.5827	11.5449	11.5353	11.5327	11.5323	20.3213	16.6103	15.5410	15.2278	15.1826
ED <sub>444</sub>	11.8046	11.7680	11.7588	11.7562	11.7559	20.3260	16.6160	15.5470	15.2340	15.1887
ED <sub>222</sub>	12.5665	12.5341	12.5260	12.5237	12.5234	20.3386	16.6314	15.5635	15.2508	15.2056
ED <sub>111</sub>	12.6355	12.6038	12.5959	12.5936	12.5933	20.4061	16.7144	15.6523	15.3414	15.2965
<i>Present models DM-E<sup>b</sup></i>										
LD <sub>555</sub>	11.5149	11.4718	11.4610	11.4579	11.4575	20.3246	16.6099	15.5394	15.2259	15.1805
LD <sub>111</sub>	11.6366	11.5942	11.5835	11.5805	11.5801	20.3345	16.6220	15.5522	15.2390	15.1937
EDZ <sub>888</sub>	11.5161	11.4725	11.4615	11.4584	11.4580	20.3264	16.6119	15.5394	15.2259	15.1805
EDZ <sub>333</sub>	11.5190	11.4752	11.4642	11.4611	11.4607	20.3250	16.6100	15.5394	15.2259	15.1806
ED <sub>999</sub>	11.5898	11.5466	11.5358	11.5327	11.5323	20.3264	16.6119	15.5414	15.2279	15.1826
ED <sub>444</sub>	11.8116	11.7698	11.7593	11.7563	11.7559	20.3310	16.6175	15.5474	15.2341	15.1887
ED <sub>222</sub>	12.5732	12.5358	12.5264	12.5238	12.5234	20.3437	16.6175	15.5639	15.2509	15.2056
ED <sub>111</sub>	12.6424	12.6056	12.5963	12.5937	12.5933	20.4113	16.7160	15.6527	15.3415	15.2965

<sup>a</sup> C-E (Complete equations).

<sup>b</sup> DM-E (Donnell–Mushtari’s shallow shell-type equations).

When the trial functions in Eq. (46) are used as solution functions in Eq. (41) along with the condition  $\tilde{C}_{16} = \tilde{C}_{26} = \tilde{C}_{36} = \tilde{C}_{45} = 0$  (condition fulfilled for cross-ply lamination schemes) the Navier-type closed-form solution is obtained. Then when cross-ply stacking sequences are investigated, the present HTRF leads to the Navier-type closed-form solution. This phenomenon is usually referred to as one-term Ritz solution. The results will be given using the usual acronyms system used in the CUF [27,30]. Therefore, the equivalent single layer theories are indicated as  $ED_{N_{u_z}N_{u_\beta}N_{u_z}}$ , where E means the equivalent single layer approach,

$D$  means that the principle of virtual displacements has been employed and  $N_{u_z}, N_{u_\beta}, N_{u_z}$  are the three different expansion orders used in the displacement field. Similarly the acronym used to describe the zig-zag theories is  $EDZ_{N_{u_z}N_{u_\beta}N_{u_z}}$ , where Z states that Murakami’s zig-zag function has been introduced. Layer-wise theories are defined as  $LD_{N_{u_z}N_{u_\beta}N_{u_z}}$  where L indicates that a layer-wise approach has been used. As highlighted in Section 6, the governing differential equations for layer-wise shell models are written for each  $k$  layer. It becomes necessary for the shell structures to have the same product  $d\alpha^* d\beta^*$  in each governing equation at  $k$ -layer

**Table 7**

Dimensionless fundamental circular frequency parameter  $\hat{\omega} = \omega a^2 \sqrt{\frac{\rho}{E_2}}$ , of square cross-ply shallow spherical shells ( $R_\beta = R_\alpha = R$ ) with stacking sequence  $[0^\circ/90^\circ/0^\circ]$ .

a/h	10					100					
	Theory	5	10	20	50	100	5	10	20	50	100
R/a											
WLC		12.417	12.227	12.179	12.165	12.164	31.022	20.359	16.632	15.426	15.246
RBF		12.063	11.861	11.810	11.796	11.794	31.216	20.394	16.595	15.361	15.176
SRBC		12.1253	11.9658	11.9253	11.9140	11.9123	31.1249	20.5381	16.8579	15.6714	15.4944
LWRBC		11.8732	11.7072	11.6651	11.6533	11.6516	31.0402	20.4065	16.6969	15.6714	15.4944
<i>Present models C-E<sup>a</sup></i>											
LD <sub>555</sub>		11.6813	11.5140	11.6392	11.6274	11.4579	30.9822	20.3325	16.6104	15.4058	15.2259
LD <sub>111</sub>		11.8004	11.6357	11.5939	11.5822	11.5805	30.9889	20.3424	16.6224	15.4187	15.2390
EDZ <sub>888</sub>		11.6856	11.5155	11.4723	11.4602	11.4584	30.9830	20.3328	16.6105	15.4058	15.2259
EDZ <sub>333</sub>		11.6889	11.5183	11.4750	11.4628	11.4611	30.9833	20.3329	16.6105	15.4058	15.2259
ED <sub>999</sub>		11.7573	11.5891	11.5464	11.5344	11.5327	30.9840	20.3343	16.6123	15.4078	15.2279
ED <sub>444</sub>		11.9734	11.8108	11.7696	11.7580	11.7563	30.9870	20.3389	16.6180	15.4139	15.2340
ED <sub>222</sub>		12.7173	12.5723	12.5356	12.5253	12.5238	30.9955	20.3516	16.6334	15.4305	15.2509
ED <sub>111</sub>		12.7850	12.6416	12.6053	12.5951	12.5937	31.0397	20.4194	16.7165	15.5201	15.3414
<i>Present models DM-E<sup>b</sup></i>											
LD <sub>555</sub>		11.7246	11.5251	11.4743	11.4601	11.4580	31.0135	20.3470	16.6137	15.4064	15.2304
LD <sub>111</sub>		11.8443	11.6469	11.5967	11.5826	11.5806	31.0172	20.3532	16.6257	15.4193	15.2390
EDZ <sub>888</sub>		11.7286	11.5265	11.4751	11.4629	11.4585	31.0123	20.3437	16.6138	15.4064	15.2260
EDZ <sub>333</sub>		11.7318	11.5293	11.4778	11.4633	11.4612	31.0116	20.3438	16.6138	15.4064	15.2260
ED <sub>999</sub>		11.8006	11.6002	11.5492	11.5349	11.5328	31.0123	20.3452	16.6156	15.4084	15.2280
ED <sub>444</sub>		12.0175	11.8221	11.7724	11.7584	11.7564	31.0153	20.3498	16.6213	15.4145	15.2342
ED <sub>222</sub>		12.7646	12.5845	12.5386	12.5257	12.5239	31.0238	20.3625	16.6367	15.4311	15.2510
ED <sub>111</sub>		12.8325	12.6538	12.6084	12.5956	12.5938	31.0686	20.4305	16.7198	15.5207	15.3416

<sup>a</sup> C-E (Complete equations).

<sup>b</sup> DM-E (Donnell-Mushtari's shallow shell-type equations).

**Table 8**

First five dimensionless circular frequency parameters  $\hat{\omega} = \omega a^2 \sqrt{\frac{\rho E_2}{h^2}}$ , of square cross-ply deep cylindrical shells with staking sequence  $[0^\circ/90^\circ/90^\circ/0^\circ]$  and  $R_\beta/a = 0.5$ .

a/h	Theory	Circular frequency parameters					Ave. err. (%)	Max err. (%)	
		$\hat{\omega}_1$	$\hat{\omega}_2$	$\hat{\omega}_3$	$\hat{\omega}_4$	$\hat{\omega}_5$			
10	3D FEM	14.840	17.468	29.094	32.464	33.046			
	FSDT	15.241	17.996	29.487	34.866	34.951	(4.05)	(7.40)	
	FSDTQ	15.250	17.989	29.491	34.795	34.913	(3.99)	(7.18)	
	<i>Present models C-E<sup>a</sup></i>								
	LD <sub>555</sub>	14.8240	17.4374	29.0603	32.3942	33.0044	(-0.15)	(-0.22)	
	LD <sub>333</sub>	14.8240	17.4374	29.0610	32.3945	33.0046	(-0.15)	(-0.21)	
	EDZ <sub>888</sub>	14.8418	17.4835	29.1475	32.4732	33.0500	(0.07)	(0.19)	
	EDZ <sub>333</sub>	14.8484	17.5197	29.3073	32.5308	33.0936	(0.29)	(0.73)	
	ED <sub>999</sub>	14.8830	17.5443	29.2259	32.7203	33.2385	(0.51)	(0.79)	
	ED <sub>444</sub>	15.0100	17.7334	29.4665	33.3910	33.7511	(1.79)	(2.86)	
	ED <sub>222</sub>	15.4550	18.4090	30.4792	36.1883	36.5010	(7.24)	(11.47)	
	ED <sub>111</sub>	15.4782	18.5796	30.7883	36.2306	36.6532	(7.80)	(11.60)	
	20	3D FEM	22.924	25.840	35.668	50.360	56.448		
		FSDT	23.177	25.959	35.925	52.769	58.869	(2.27)	(4.78)
		FSDTQ	23.178	25.978	35.923	52.746	57.077	(1.64)	(4.74)
<i>Present models C-E<sup>a</sup></i>									
LD <sub>555</sub>		22.9119	25.8360	35.6696	50.3126	56.4101	(-0.05)	(-0.09)	
LD <sub>333</sub>		22.9119	25.8360	35.6696	50.3126	56.4102	(-0.05)	(-0.09)	
EDZ <sub>888</sub>		22.9334	25.8395	35.7063	50.3655	56.4728	(0.04)	(0.11)	
EDZ <sub>333</sub>		22.9454	25.8438	35.7736	50.3841	56.5233	(0.12)	(0.30)	
ED <sub>999</sub>		22.9620	25.8539	35.7447	50.6122	56.7346	(0.29)	(0.51)	
ED <sub>444</sub>		23.0518	25.8990	35.8761	51.3614	57.1918	(0.94)	(1.99)	
ED <sub>222</sub>		23.3229	26.0345	36.3267	53.9564	58.0846	(2.88)	(7.14)	
ED <sub>111</sub>		23.5325	26.0551	36.8524	54.1642	58.9083	(3.74)	(7.55)	

<sup>a</sup> C-E (Complete equations).

level due to the curvature variations. This operation can be undertaken choosing the value on the reference shell surface  $\Omega$ ,  $d\alpha d\beta$  as  $d\alpha^* d\beta^*$ . Then, each  $d\alpha_k d\beta_k$  defined on  $\Omega_k$  can therefore be written as:

$$d\alpha_k d\beta_k = \frac{R_\alpha R_\beta}{R_\alpha^k R_\beta^k} d\alpha d\beta \quad (47)$$

The proposed advanced shell models have been assessed by comparison with the 3D elasticity solution and other results present in literature and listed in Table 1.

### 7.1. Cross-ply laminated hollow circular cylindrical shells

A preliminary assessment of the CUF-based equivalent single layer, zig-zag and layer-wise theories is undertaken in Tables 3–5, respectively. Simply-supported cross-ply circular cylindrical shells with material Mat-1 given in Table 2 are studied. Results are compared towards the exact 3D elasticity solution provided by Ye and Soldatos [88] and other theories from the literature. The theories PAR<sub>ds</sub>, HYT<sub>ds</sub>, UNI<sub>cs</sub>, PAR<sub>cs</sub> and HYT<sub>cs</sub> are given by Timarci and Soldatos [89], in particular PAR<sub>ds</sub> and HYT<sub>ds</sub> account

for a parabolic and hyperbolic discontinuous distribution of the interlaminar stresses, respectively. In sharp contrast, the theories  $UNI_{cs}$ ,  $PAR_{cs}$  and  $HYT_{cs}$  have a uniform, parabolic and hyperbolic continuous distribution of the interlaminar stresses, respectively. Further theories considered for comparison purpose are the refined zig-zag theory ZZD given by Di Sciuva and Carrera [90] and the refined higher order model provided by Matsunaga [91]. As can be seen from Tables 3 and 4 equivalent single layer and zig-zag shell modes provide accurate results in terms of average and maximum error percentages of the first six dimensionless circular frequency parameters if at least a cubic expansions is used. Indeed, in this last case for equivalent single layer shell models average and maximum error percentages are 1.5265% and 1.5705%, respectively, when using the complete shell equations (C-E), whilst 1.5374% and 1.5705% when applying the Donnell-Mushtari's shallow shell-type equations (DM-E). The introduction of the Murakami zig-zag function (MZZF) in the equivalent single layer displacement field does not affect considerably the results, both in the case of C-E, where the error percentages are 1.5254% and 1.5693%, and in the case of DM-E where their values are 1.5362% and 1.5693%, respectively. In the same Tables, it is interesting to note that if a higher accuracy is required, in both cases the fifth order is needed, indeed in this case the average and maximum error percentages are lower than the 1%. Layer-wise shell models have been assessed in Table 5. As can be seen in the same Table, by using a cubic trend of the displacement components at each layer through the thickness and the C-E, the solution perfectly matches the 3D exact one. A similar observation can be drawn when applying the DM-E, although in this case, as expected, for lower values of the radius-to-length ratio small error percentages can be observed.

7.2. Cross-ply laminated shallow cylindrical and spherical shells

Simply-supported three-layered cross-ply shallow cylindrical and spherical shells made of Mat-1 (see Table 2) are analyzed in Tables 6 and 7. The results, obtained by using the advanced shell models, are presented in terms of dimensionless fundamental circular frequency parameter and are in good agreement with those proposed by Ferreira et al. [59,60,92,93] by using different solution methods such as wavelet collocation, radial basis, sinusoidal radial basis collocation and layer-wise radial basis collocation, respectively. With respect to the circular cylindrical shell case, the use of the MZZF introduces a conspicuous refinement in results above all when thick shallow shells are analyzed. DM-E in this case lead to a similar accuracy of the C-E.

7.3. Cross-ply laminated deep cylindrical shells

In Table 8 the developed shell models are used to compute the first five dimensionless circular frequency parameters of four-layers symmetric cross-ply deep thick and moderately thick cylindrical shells made of Mat-1 (see Table 2). The accuracy of the present models, in terms of average and maximum error percentages, is proved by comparison with a 3D FEM solution [58] and other theories present in literature [58]. As can be seen from the Table 8 the present higher order equivalent single layer, zig-zag and layer-wise shell models provide a better accuracy compared to the FSDT, based on plate-like stiffness coefficients, and the FSDTQ by Qatu [58], where the stiffness coefficients have been integrated exactly. In particular, for  $a/h = 10$  the shell models  $ED_{999}$ ,  $EDZ_{333}$ ,  $EDZ_{888}$ ,  $LD_{333}$  and  $LD_{555}$  lead to an average error percentage which is equal or lower than the 0.5% against the 4% of the aforementioned FSDT. A similar behavior can be observed for  $a/h = 20$  in this case the average error percentage for the models  $EDZ_{333}$ ,  $EDZ_{888}$ ,  $LD_{333}$  and  $LD_{555}$  is equal or lower than the 0.1%. In the authors opinion, the results obtained represent a further confirmation of the

**Table 9**  
Convergence analysis of the first six dimensionless circular frequency parameters  $\hat{\omega} = \omega \sqrt{\frac{\rho^* h^3}{E_1}}$  of square angle-ply shallow cylindrical shells with lamination scheme  $[30^\circ / -30^\circ / 30^\circ]$ ,  $a/h = 20$ ,  $R_0/a = 2$  and varying ED shell models.

Theory	M, N	Circular frequency parameters					
		$\hat{\omega}_1$	$\hat{\omega}_2$	$\hat{\omega}_3$	$\hat{\omega}_4$	$\hat{\omega}_5$	$\hat{\omega}_6$
ED <sub>222</sub>	2	6.05979	10.5638	13.4782	18.6496	41.3612	66.7889
	4	6.04580	10.4567	13.3512	17.8015	20.2029	24.6456
	6	6.03959	10.4387	13.3324	17.7464	20.1729	24.6136
	8	6.03603	10.4305	13.3241	17.7251	20.1605	24.6019
	10	6.03369	10.4257	13.3193	17.7134	20.1534	24.5955
ED <sub>444</sub>	2	6.05555	10.5397	13.4419	18.5691	41.3611	66.7883
	4	6.04142	10.4334	13.3159	17.7334	20.1147	24.5033
	6	6.03507	10.4155	13.2971	17.6787	20.0850	24.4718
	8	6.03137	10.4073	13.2888	17.6574	20.0728	24.4602
	10	6.02890	10.4025	13.2839	17.6458	20.0658	24.4539
ED <sub>666</sub>	2	6.05548	10.5397	13.4419	18.5690	41.3611	66.7881
	4	6.04131	10.4333	13.3157	17.7331	20.1145	24.5031
	6	6.03491	10.4154	13.2969	17.6783	20.0849	24.4715
	8	6.03117	10.4072	13.2886	17.6570	20.0726	24.4599
	10	6.02867	10.4024	13.2837	17.6453	20.0656	24.4536
ED <sub>888</sub>	2	6.05546	10.5397	13.4419	18.5690	41.3611	66.7881
	4	6.04127	10.4333	13.3157	17.7329	20.1145	24.5030
	6	6.03487	10.4153	13.2969	17.6781	20.0848	24.4714
	8	6.03112	10.4071	13.2885	17.6567	20.0725	24.4597
	10	6.02860	10.4023	13.2836	17.6450	20.0654	24.4534
12	6.02677	10.3990	13.2803	17.6375	20.0607	24.4494	

importance of develop shell theories, which account for not only of a correct description of the curvature terms and higher order expansion in the displacement model but also of the zig-zag trend of the displacement components through the thickness due to the transverse anisotropy of laminated composite structures.

**Table 10**  
Convergence analysis of the first six dimensionless circular frequency parameters  $\hat{\omega} = \omega \sqrt{\frac{\rho^* h^3}{E_1}}$  of square angle-ply shallow cylindrical shells with lamination scheme  $[30^\circ / -30^\circ / 30^\circ]$ ,  $a/h = 20$ ,  $R_0/a = 2$  and varying LD shell models.

Theory	M,N	Circular frequency parameters					
		$\hat{\omega}_1$	$\hat{\omega}_2$	$\hat{\omega}_3$	$\hat{\omega}_4$	$\hat{\omega}_5$	$\hat{\omega}_6$
LD <sub>111</sub>	2	6.06721	10.5827	13.4860	18.6539	41.3603	66.7860
	4	6.05341	10.4768	13.3606	17.8179	20.2188	24.6287
	6	6.04727	10.4590	13.3420	17.7633	20.1893	24.5972
	8	6.04374	10.4509	13.3338	17.7421	20.1771	24.5856
	10	6.04142	10.4461	13.3290	17.7306	20.1701	24.5794
LD <sub>222</sub>	2	6.03975	10.4429	13.3259	17.7232	20.1654	24.5754
	4	6.03975	10.4429	13.3259	17.7232	20.1654	24.5754
	6	6.05565	10.5395	13.4416	18.5689	41.3602	66.7853
	8	6.04160	10.4332	13.3159	17.7335	20.1142	24.5039
	10	6.03525	10.4153	13.2972	17.6788	20.0846	24.4725
LD <sub>333</sub>	2	6.03154	10.4071	13.2889	17.6575	20.0723	24.4608
	4	6.02905	10.4022	13.2840	17.6459	20.0653	24.4545
	6	6.02723	10.3990	13.2807	17.6384	20.0606	24.4505
	8	6.05559	10.5392	13.4412	18.5679	41.3602	66.7853
	10	6.04153	10.4328	13.3155	17.7324	20.1131	24.5020
LD <sub>444</sub>	2	6.03518	10.4149	13.2967	17.6776	20.0834	24.4705
	4	6.03146	10.4067	13.2883	17.6563	20.0711	24.4588
	6	6.02897	10.4018	13.2834	17.6446	20.0641	24.4525
	8	6.02714	10.3986	13.2802	17.6371	20.0594	24.4485
	10	6.05559	10.5392	13.4412	18.5679	41.3601	66.7853
LD <sub>555</sub>	2	6.04153	10.4328	13.3154	17.7324	20.1131	24.5020
	4	6.03518	10.4149	13.2967	17.6776	20.0834	24.4705
	6	6.03146	10.4067	13.2883	17.6563	20.0711	24.4588
	8	6.02897	10.4018	13.2835	17.6446	20.0641	24.4525
	10	6.02714	10.3986	13.2802	17.6371	20.0594	24.4485



**Table 11**

The first six dimensionless circular frequency parameters  $\hat{\omega} = \omega \sqrt{\frac{\rho^*}{E_1 h^3}}$  of square angle-ply shallow cylindrical shells with lamination scheme  $[\theta^\circ / -\theta^\circ / \theta^\circ]$ ,  $a/h = 20$ ,  $R_\beta/a = 2$  and varying lamination angle.

$\theta$	Theory	Circular frequency parameters					
		$\hat{\omega}_1$	$\hat{\omega}_2$	$\hat{\omega}_3$	$\hat{\omega}_4$	$\hat{\omega}_5$	$\hat{\omega}_6$
0	R-FSDT	5.601	11.71	13.05	18.10	20.69	27.09
	Present models						
	ED <sub>222</sub>	5.56160	9.61671	13.6096	17.4397	18.1951	25.2084
	ED <sub>888</sub>	5.55789	9.59923	13.5670	17.3712	18.1358	25.0820
	LD <sub>444</sub>	5.55769	9.59862	13.5664	17.3703	18.1346	25.0805
15	R-FSDT	5.759	11.92	12.96	18.24	21.20	27.11
	Present models						
	ED <sub>222</sub>	5.72046	9.85614	13.5277	17.4717	18.7924	25.5647
	ED <sub>888</sub>	5.71605	9.83681	13.4871	17.4053	18.7229	25.4308
	LD <sub>444</sub>	5.71610	9.83630	13.4868	17.4046	18.7216	25.4295
30	R-FSDT	6.073	11.89	13.05	18.48	22.44	25.44
	Present models						
	ED <sub>222</sub>	6.03202	10.4224	13.3160	17.7060	20.1487	24.5916
	ED <sub>888</sub>	6.02677	10.3990	13.2803	17.6375	20.0607	24.4494
	LD <sub>444</sub>	6.02714	10.3986	13.2802	17.6371	20.0594	24.4485
45	R-FSDT	6.252	11.35	13.37	18.60	23.17	24.38
	Present models						
	ED <sub>222</sub>	6.17965	11.0546	13.0625	17.8932	21.8150	23.0290
	ED <sub>888</sub>	6.17423	11.0271	13.0312	17.8226	21.7060	22.9161
	LD <sub>444</sub>	6.17468	11.0267	13.0310	17.8222	21.7045	22.9150
60	R-FSDT	6.097	10.70	13.65	18.39	21.26	26.16
	Present models						
	ED <sub>222</sub>	5.99515	11.5873	12.7358	17.7978	21.4042	23.7793
	ED <sub>888</sub>	5.98997	11.5583	12.7056	17.7276	21.3236	23.6327
	LD <sub>444</sub>	5.99036	11.5582	12.7049	17.7272	21.3229	23.6308
75	R-FSDT	5.785	10.11	13.90	18.16	19.75	27.16
	Present models						
	ED <sub>222</sub>	5.66967	11.6855	12.5157	17.5282	20.3073	25.2042
	ED <sub>888</sub>	5.66533	11.6664	12.4748	17.4594	20.2459	25.0252
	LD <sub>444</sub>	5.66541	11.6665	12.4737	17.4587	20.2451	25.0234
90	R-FSDT	5.626	9.863	14.00	18.11	19.11	26.70
	Present models						
	ED <sub>222</sub>	5.50864	11.4918	12.5690	17.3860	19.8466	25.6091
	ED <sub>888</sub>	5.50502	11.4775	12.5233	17.3178	19.7928	25.4855
	LD <sub>444</sub>	5.50484	11.4770	12.5224	17.3168	19.7920	25.4842

**Table 12**

Convergence analysis of the first six dimensionless circular frequency parameters  $\hat{\omega} = \omega \sqrt{\frac{\rho^*}{E_1 h^3}}$  of square angle-ply shallow spherical shells with lamination scheme  $[30^\circ / -30^\circ / 30^\circ]$ ,  $a/h = 20$ ,  $R_\beta/a = 2$  and varying ED shell models.

Theory	M, N	Circular frequency parameters					
		$\hat{\omega}_1$	$\hat{\omega}_2$	$\hat{\omega}_3$	$\hat{\omega}_4$	$\hat{\omega}_5$	$\hat{\omega}_6$
ED <sub>222</sub>	2	9.17074	13.2518	14.1994	19.8518	41.1268	66.6311
	4	9.15951	13.1654	14.0939	19.1525	21.7407	24.7567
	6	9.15401	13.1497	14.0770	19.0988	21.7156	24.7249
	8	9.15067	13.1426	14.0691	19.0777	21.7049	24.7131
	10	9.14838	13.1384	14.0643	19.0662	21.6986	24.7067
	12	9.14667	13.1356	14.0611	19.0587	21.6944	24.7027
ED <sub>444</sub>	2	9.16756	13.2326	14.1654	19.7765	41.1266	66.6305
	4	9.15588	13.1464	14.0609	19.0882	21.6602	24.6155
	6	9.14997	13.1306	14.0440	19.0347	21.6355	24.5835
	8	9.14625	13.1234	14.0360	19.0136	21.6249	24.5725
	10	9.14360	13.1191	14.0311	19.0019	21.6186	24.5661
	12	9.14156	13.1161	14.0277	18.9944	21.6144	24.5621
ED <sub>666</sub>	2	9.16741	13.2326	14.1654	19.7765	41.1266	66.6304
	4	9.15562	13.1463	14.0608	19.0879	21.6601	24.6153
	6	9.14962	13.1304	14.0438	19.0342	21.6353	24.5839
	8	9.14583	13.1231	14.0358	19.0131	21.6246	24.5722
	10	9.14310	13.1187	14.0308	19.0013	21.6183	24.5658
	12	9.14099	13.1157	14.0274	18.9937	21.6140	24.5618
ED <sub>888</sub>	2	9.16737	13.2326	14.1654	19.7765	41.1266	66.6303
	4	9.15556	13.1462	14.0607	19.0877	21.6600	24.6152
	6	9.14955	13.1303	14.0437	19.0340	21.6352	24.5837
	8	9.14574	13.1230	14.0357	19.0128	21.6245	24.5720
	10	9.14301	13.1186	14.0307	19.0010	21.6182	24.5656
	12	9.14088	13.1156	14.0273	18.9934	21.6139	24.5616

**Table 13**

Convergence analysis of the first six dimensionless circular frequency parameters  $\hat{\omega} = \omega \sqrt{\frac{\rho^*}{E_1 h^3}}$  of square angle-ply shallow spherical shells with lamination scheme  $[30^\circ / -30^\circ / 30^\circ]$ ,  $a/h = 20$ ,  $R_\beta/a = 2$  and varying LD shell models.

Theory	M, N	Circular frequency parameters					
		$\hat{\omega}_1$	$\hat{\omega}_2$	$\hat{\omega}_3$	$\hat{\omega}_4$	$\hat{\omega}_5$	$\hat{\omega}_6$
LD <sub>111</sub>	2	9.17478	13.2660	14.2034	19.8523	41.1229	66.6248
	4	9.16380	13.1811	14.1000	19.1648	21.7539	24.7351
	6	9.15841	13.1657	14.0835	19.1118	21.7294	24.7039
	8	9.15513	13.1588	14.0757	19.0911	21.7189	24.6923
	10	9.15286	13.1547	14.0710	19.0796	21.7127	24.6860
	12	9.15115	13.1519	14.0678	19.0723	21.7086	24.6821
LD <sub>222</sub>	2	9.16707	13.2319	14.1620	19.7731	41.1228	66.6241
	4	9.15558	13.1465	14.0584	19.0871	21.6571	24.6118
	6	9.14972	13.1308	14.0416	19.0339	21.6324	24.5806
	8	9.14599	13.1236	14.0337	19.0129	21.6218	24.5690
	10	9.14331	13.1193	14.0288	19.0012	21.6155	24.5626
	12	9.14122	13.1163	14.0254	18.9936	21.6113	24.5586
LD <sub>333</sub>	2	9.16703	13.2316	14.1616	19.7721	41.1228	66.6241
	4	9.15553	13.1462	14.0580	19.0860	21.6560	24.6099
	6	9.14967	13.1305	14.0412	19.0327	21.6313	24.5787
	8	9.14594	13.1233	14.0332	19.0117	21.6207	24.5670
	10	9.14325	13.1189	14.0283	19.0000	21.6144	24.5607
	12	9.14116	13.1160	14.0249	18.9924	21.6102	24.5566
LD <sub>444</sub>	2	9.16703	13.2316	14.1616	19.7721	41.1228	66.6241
	4	9.15553	13.1462	14.0580	19.0860	21.6560	24.6099
	6	9.14967	13.1305	14.0412	19.0327	21.6313	24.5787
	8	9.14594	13.1233	14.0332	19.0117	21.6207	24.5670
	10	9.14325	13.1190	14.0283	19.0000	21.6144	24.5607
	12	9.14116	13.1160	14.0249	18.9924	21.6102	24.5566

**Table 14**

The first six dimensionless circular frequency parameters  $\hat{\omega} = \omega \sqrt{\frac{a^4 \rho}{E_1 h^3}}$ , of square angle-ply shallow spherical shells with lamination scheme  $[\theta^\circ / -\theta^\circ / \theta^\circ]$ ,  $a/h = 20$ ,  $R_\beta/a = 2$  and varying lamination angle.

$\theta$	Theory	Circular frequency parameters					
		$\hat{\omega}_1$	$\hat{\omega}_2$	$\hat{\omega}_3$	$\hat{\omega}_4$	$\hat{\omega}_5$	$\hat{\omega}_6$
0	R-FSDT	8.238	12.70	14.53	19.10	21.05	27.63
	Present models						
	ED <sub>222</sub>	8.16239	12.4679	14.0675	18.3990	20.1737	26.1735
	ED <sub>888</sub>	8.15995	12.4546	14.0268	18.3345	20.1208	26.0524
15	LD <sub>444</sub>	8.15891	12.4526	14.0241	18.3309	20.1170	26.0472
	R-FSDT	8.566	13.00	14.48	19.32	21.56	27.89
	Present models						
	ED <sub>222</sub>	8.49490	12.7660	14.0470	18.6266	20.6314	25.9976
30	ED <sub>888</sub>	8.49083	12.7503	14.0083	18.5618	20.5703	25.8244
	LD <sub>444</sub>	8.49041	12.7494	14.0059	18.5596	20.5665	25.8193
	R-FSDT	9.209	13.38	14.44	19.74	22.78	26.35
	Present models						
45	ED <sub>222</sub>	9.14667	13.1356	14.0611	19.0587	21.6944	24.7027
	ED <sub>888</sub>	9.14088	13.1156	14.0273	18.9934	21.6139	24.5616
	LD <sub>444</sub>	9.14116	13.1159	14.0249	18.9924	21.6102	24.5566
	R-FSDT	9.542	13.44	14.45	19.93	24.10	24.82
Present models	ED <sub>222</sub>	9.48738	13.1849	14.1088	19.2669	23.4617	27.5087
	ED <sub>888</sub>	9.48125	13.1635	14.0772	19.2011	22.6695	23.3465
	LD <sub>444</sub>	9.48164	13.1638	14.0750	19.2002	22.6660	23.3410

**Table 15**

The first six dimensionless circular frequency parameters  $\hat{\omega} = \omega \sqrt{\frac{a^4 \rho}{E_1 h^3}}$ , of square angle-ply deep cylindrical shells with lamination scheme  $[\theta^\circ / -\theta^\circ / \theta^\circ]$ ,  $a/h = 20$ ,  $R_\beta/a = 1$  and varying lamination angle.

$\theta$	Theory	Circular frequency parameters					
		$\hat{\omega}_1$	$\hat{\omega}_2$	$\hat{\omega}_3$	$\hat{\omega}_4$	$\hat{\omega}_5$	$\hat{\omega}_6$
0	R-FSDT	8.105	10.21	16.58	19.02	19.15	26.94
	Present models						
	ED <sub>222</sub>	7.99623	9.79936	16.1853	18.0428	18.2572	25.3111
	ED <sub>888</sub>	7.99387	9.78281	16.1505	17.9839	18.1931	25.1869
15	LD <sub>444</sub>	7.99327	9.78061	16.1480	17.9790	18.1897	25.1812
	R-FSDT	8.428	10.48	16.66	18.99	19.96	27.42
	Present models						
	ED <sub>222</sub>	8.31800	10.0571	16.2740	18.0826	18.9341	25.7251
30	ED <sub>888</sub>	8.31404	10.0385	16.2405	18.0225	18.8629	25.5937
	LD <sub>444</sub>	8.31405	10.0367	16.2390	18.0191	18.8591	25.5889
	R-FSDT	9.040	11.10	16.82	19.43	21.47	28.25
	Present models						
45	ED <sub>222</sub>	8.92476	10.6345	16.4766	18.5481	20.2279	26.5429
	ED <sub>888</sub>	8.91916	10.6114	16.4476	18.4840	20.1404	26.3988
	LD <sub>444</sub>	8.92476	10.6345	16.4766	18.5481	20.2279	26.5429
	R-FSDT	9.301	11.79	17.10	19.83	23.38	26.89
60	Present models						
	ED <sub>222</sub>	9.17254	11.2519	16.8032	18.9613	21.8101	25.6224
	ED <sub>888</sub>	9.16674	11.2231	16.7799	18.8943	21.6987	25.5270
	LD <sub>444</sub>	9.16781	11.2212	16.7791	18.8933	21.6925	25.5236
75	R-FSDT	8.917	12.45	17.16	19.71	25.40	25.99
	Present models						
	ED <sub>222</sub>	8.76526	11.8160	16.8986	9.5530	18.8270	23.5073
	ED <sub>888</sub>	8.75989	11.7807	16.8802	9.3873	18.7595	23.3640
90	LD <sub>444</sub>	8.76097	11.7787	16.8793	9.3376	18.7588	23.3572
	R-FSDT	8.284	12.97	16.56	19.24	25.21	27.13
	Present models						
	ED <sub>222</sub>	8.11334	12.2461	16.2923	18.3234	24.3404	24.9186
Present models	ED <sub>888</sub>	8.10965	12.2047	16.2791	18.2584	24.2907	24.7417
	LD <sub>444</sub>	8.11004	12.2022	16.2778	18.2564	24.2875	24.7347
	R-FSDT	7.968	13.17	16.09	18.97	24.81	27.77
	Present models						
90	ED <sub>222</sub>	7.79085	12.4158	15.8134	18.0488	23.9632	25.4610
	ED <sub>888</sub>	7.78871	12.3715	15.8039	17.9858	23.9208	25.2689
	LD <sub>444</sub>	7.78850	12.3684	15.8023	17.9824	23.9174	25.2621

#### 7.4. Angle-ply laminated shallow cylindrical and spherical shells

In Tables 9–11 moderately thick and symmetric angle-ply laminated shallow cylindrical shells are investigated. A convergence analysis of the first six dimensionless frequency parameters taking into account a stacking sequence  $[30^\circ / -30^\circ / 30^\circ]$ , length-to-thickness ratio  $a/h = 20$ , radius-to-length ratio  $R_\beta/a = 2$  and Mat-2 (see Table 2) is carried out by exploiting the use of ED and LD shell models. Both the kinematics descriptions (equivalent single layer, zig-zag and layer-wise) and the higher order terms do not affect the rate of convergence. From an overall point of view, the conver-

gence towards the exact one is quite quick and smooth, this is due to the choice of the trigonometric trial functions, which has stated and proved in [30], show a stable behavior even at higher half-wave numbers. In Table 11, results obtained taking into account a three-layered regular symmetric angle-ply  $[\theta^\circ / -\theta^\circ / \theta^\circ]$  having the same geometrical and material properties aforementioned, varying the lamination angle in a range starting from  $0^\circ$  to  $90^\circ$  with  $15^\circ$  increments, using half-wave numbers  $M = N = 12$  and employing the shell models ED<sub>222</sub>, ED<sub>888</sub>, LD<sub>444</sub> are compared with those provided by Qatu [94] using algebraic polynomial trial functions (108 DOFs). An excellent agreement is found for the fundamental

dimensionless circular frequency parameter the difference increases when increasing the frequency. In Tables 12–14 the same investigation is performed for moderately thick and symmetric angle-ply laminated shallow spherical shells. By virtue of the second curvature  $R_\alpha$  along the  $\alpha$  direction (see Fig. 1) which increases the global stiffness of the structure the dimensionless circular frequency parameters are higher with respect to the previous case (cylindrical shells). Both for the convergence analysis undertaken in Tables 12, 13 and for the direct comparison of the results with those proposed by Qatu in Table 14 can be formulated similar considerations stated in the case of shallow cylindrical shells. However for spherical shells the investigation of the lamination angle range can be restricted from  $0^\circ$  to  $45^\circ$  due to the geometrical symmetry of the structures.

### 7.5. Angle-ply laminated deep cylindrical shells

In Table 15 the first six dimensionless frequency parameters of moderately thick and symmetric angle-ply laminated deep cylindrical shells made of Mat-2, with stacking sequence  $[\theta^\circ / -\theta^\circ / \theta^\circ]$ , lamination angle varying from  $0^\circ$  to  $90^\circ$  with  $15^\circ$  increments, length-to-thickness ratio  $a/h = 20$ , radius-to-length ratio  $R_\beta/a = 1$ , half-wave numbers  $M = N = 12$  and by using the shell models ED<sub>222</sub>, ED<sub>888</sub>, LD<sub>444</sub> are compared with those provided by Qatu [94]. Once again an excellent agreement is found for the dimensionless fundamental circular frequency parameter, but taking into account higher frequencies the differences increase. With respect to shallow cylindrical shells having the same geometrical and material properties the frequency are higher and comparable to those of shallow spherical shells.

## 8. Conclusions

The hierarchical trigonometric Ritz formulation for the first time has been extended to shell structures in order to perform free vibration analysis of doubly-curved anisotropic laminated composite shallow and deep shells. Refined higher order equivalent single layer, zig-zag and layer-wise shell models are assessed by comparison with the 3D elasticity and 3D FEM solutions. Several shell geometries accounting for thin and thick shallow cylindrical and spherical shells, deep cylindrical shells and hollow circular cylindrical shells, with cross-ply and angle-ply stacking sequences have been investigated. The influence of kinematics descriptions and higher order terms on the rate of convergence have been examined. The effects of significant parameters such as stacking sequence, length-to-thickness ratio and radius-to-length ratio on the circular frequency parameters have been discussed. From the analyses carried out the following conclusions can be drawn:

- The hierarchical shell models provide the best results in terms of dimensionless circular frequency parameters when compared to those present in literature or obtained by virtue of commercial FEM softwares.
- The full description of curvature terms and higher order terms are needed in order to improve the accuracy.
- Layer-wise and zig-zag theories, which account for the zig-zag trend of the displacement components through the thickness due to the transverse anisotropy, are compulsory when thick deep cylindrical shells are analyzed.
- Layer-wise theories embedded in the HTRF lead to the 3D elasticity solution with a computational cost lower than that required by complex 3D FEM models.
- Kinematics descriptions and higher order terms do not affect the rate of convergence.

## References

- [1] Donnell LH. Stability of thin walled tubes under torsion. Tech. rep. 479, NACA; 1933.
- [2] Donnell LH. A discussion of thin shell theory. In: Proceedings of the fifth international congress for applied mechanics; 1938.
- [3] Mushtari KM. On the stability of cylindrical shells subjected to torsion. Trudy Kazanskogo aviatsionnogo inatituta 1938;2 [in Russian].
- [4] Mushtari KM. Certain generalizations of the theory of thin shells. Izv Fiz Mat Odd pri Kazan Univ 1938;11(8) [in Russian].
- [5] Love A E H. A treatise on the mathematical theory of elasticity. 4th ed. New York: Dover Pub.; 1944.
- [6] Love AEH. The small free vibrations and deformations of a thin elastic shell. Philos Trans Roy Soc (Lond) Ser A 1888(179):491–549.
- [7] Timoshenko SP. Theory of plates and shells. New York: McGraw Hill; 1959.
- [8] Gol'denveizer AL. Theory of thin shells. New York: Pergamon Press; 1961.
- [9] Novozhilov VV. The theory of thin elastic shells. Groningen (The Netherlands): P. Noordhoff Lts; 1964.
- [10] Flügge W. Statik und Dynamik der Schalen. Berlin: Julius Springer; 1934 [Reprinted by Edwards Brothers Inc., Ann Arbor, Mich., 1943].
- [11] Flügge W. Stresses in shells. Berlin: Springer Verlag; 1962.
- [12] Lu'ye AI. General theory of elastic shells. Prikl Mat Mekh 1940;4(1):7–34.
- [13] Byrne R. Theory of small deformations of a thin elastic shell. Sem Rep Math Univ Calif Pub Math NS 1944;2(1):103–52.
- [14] Reissner E. A new derivation of the equations of the deformation of elastic shells. Am J Math 1941;63(1):177–84.
- [15] Naghdi PM, Berry JG. On the equations of motion of cylindrical shells. J Appl Mech 1964;21(2):160–6.
- [16] Sanders JL. An improved first approximation theory of thin shells. Tech. rep. R24, NASA; 1959.
- [17] Vlasov VZ. Osnovnye differentsialnye uravnenia obshche teorii uprugikh obolochek. Prikl Mat Mekh 1944;8 [English translation: NACA TM 1241, Basic differential equations in the general theory of elastic shells, 1951].
- [18] Vlasov VZ. Obshchaya teoriya obolochek; yeye prilozheniya v tekhnike. Gos. Izd. Tekh.-Teor.-Lit., Moscow-Leningrad, 1949 [English translation: NASA TTF-99, General theory of shells and its applications in engineering, 1964].
- [19] Arnold RN, Warburton GB. Flexural vibrations of the walls of thin cylindrical shells having freely supported ends. Proc Roy Soc (Lond) Ser A 1949;238–56.
- [20] Arnold RN, Warburton GB. The flexural vibrations of thin cylinders. Inst Mech Eng Ser A 1953(167):62–80.
- [21] Houghton DS, Johns DJ. A comparison of the characteristic equations in the theory of circular cylindrical shells. Aeronaut Quart 1961;228–36.
- [22] Leissa WA. Vibration of shells. Tech. rep. SP-288, Washington, DC, NASA: Scientific and technical information Office; 1973.
- [23] Koiter WT. A consistent first approximations in the general theory of thin elastic shells. In: Proceedings of symposium on the theory of thin elastic shells, North-Holland Amsterdam; August 1959. p. 12–23.
- [24] Carrera E. A study of transverse normal stress effects on vibration of multilayered plates and shells. J Sound Vib 1999;225:803–29.
- [25] Carrera E. A class of two-dimensional theories for anisotropic multilayered plates analysis. Atti Accademia delle scienze Torino Memorie Scienze Fisiche 1995;19–20:49–87.
- [26] Carrera E. Theories and finite elements for multilayered anisotropic composite plates and shells. Arch Comput Methods Eng 2002;9(2):87–140.
- [27] Carrera E. Theories and finite elements for multilayered plates and shells: a unified compact formulation with numerical assessment and benchmarking. Arch Comput Methods Eng 2003;10(3):216–96.
- [28] Carrera E. Developments ideas and evaluation based upon Reissner's mixed variational theorem in the modeling of multilayered plates and shells. Appl Mech Rev 2001;54:301–29.
- [29] Carrera E. A Reissner's mixed variational theorem applied to vibration analysis of multilayered shells. J Appl Mech 1999;66:69–78.
- [30] Fazzolari FA, Carrera E. Accurate free vibration analysis of thermo-mechanically pre/post-buckled anisotropic multilayered plates based on a refined hierarchical trigonometric Ritz formulation. Compos Struct 2013;95:381–402.
- [31] Carrera E, Petrolo M. Guidelines and recommendations to construct theories for metallic and composite plates. AIAA J 2010;48:2852–66.
- [32] Denis ST, Palazotto AN. Transverse shear deformation in orthotropic cylindrical pressure vessels using a higher-order shear deformation theory. AIAA J 1989;27(10):1441–7.
- [33] Di S, Ramm E. Hybrid stress formulation for higher-order theory of laminated shell analysis. Comput Methods Appl Mech Eng 1993;109:356–9.
- [34] Bert CW. Analysis of shells. New York: L.J. Broutman, Wiley; 1980.
- [35] Librescu L. Elasto-statics and kinetics of anisotropic heterogeneous shell-type structures. 1st ed. Leyden, The Netherlands: Noordhoff International; 1975.
- [36] Grigolyuk EI, Kulicov GM. General direction of the development of the theory of shells. Mekhanika kompozitnykh Materialov 1988;24(2):287–98.
- [37] Fettahioglu OA, Steele CR. Asymptotic solutions for orthotropic non-homogeneous shells of revolution. J Appl Mech 1974;41:753–8.
- [38] Widera GEO, Logan DL. Refined theories for non-homogeneous anisotropic, cylindrical shells: Part I – Derivation. J Eng Mech Div ACSE 1980;106:1053–7.
- [39] Widera GEO, Fan H. On the derivation of a refined theory for non-homogeneous anisotropic shells of revolution. J Appl Mech 1988;110:102–5.

- [40] Spencer AJM, Watson P, Rogers TG. Stress analysis of laminated circular cylindrical shells, in: Recent developments in composite materials structures. In: Proceedings of the symposium, ASME winter annual meeting, Dallas, TX; November 25–30, 1990. p. 57–60.
- [41] Cicala P. Systematic approach to linear shell theory. Turin, Italy: Levrotto & Bella; 1965.
- [42] Kapania RK. A review on the analysis of laminated shells. *J Press Vess Technol* 1989;111:88–96.
- [43] Noor AK, Burton WS. Assessment of computational models for multilayered composite shells. *Appl Mech Rev* 1990;43:2141–6.
- [44] Folsberg K. Influence of boundary conditions on the modal characteristics of thin cylindrical shells. *AIAA J* 1964;2(12):2150–7.
- [45] Soedel W. Simplified equations and solutions for the vibration of orthotropic cylindrical shells. *J Sound Vib* 1983;87(4):555–66.
- [46] Das YC. Vibrations of orthotropic cylindrical shells. *Appl Sci Res* 1964;12(4–5):17–26.
- [47] Dong SB. Free vibrations of laminated orthotropic cylindrical shells. *J Acoust Soc Am* 1968;44:1628–35.
- [48] Callahan J, Baruh H. A closed-form solution procedure for circular cylindrical shell vibrations. *Int J Solids Struct* 1999;36:2973–3013.
- [49] Liu B, Xing YF, Qatu MS, Ferreira AJM. Exact characteristic equations for free vibrations of thin orthotropic circular cylindrical shells. *Compos Struct* 2012;94(2):484–93.
- [50] Zhao X, Ng TY, Liew KM. Free vibration of two-side simply supported laminated cylindrical panels via the mesh-free kp-ritz method. *Int J Mech Sci* 2004;46:123–42.
- [51] Zhao X, Liew KM, Ng TY. Vibration analysis of laminated composite cylindrical panels via a meshfree approach. *Int J Solid Struct* 2003;40:161–80.
- [52] Liew KM, Lim CW. A Ritz vibration analysis of doubly-curved rectangular laminated shallow shells using a refined first-order theory. *Comput Methods Appl Mech Eng* 1995;127:145–62.
- [53] Lm CW, Liew KM. A higher order theory for vibration of shear deformable laminated shallow shells. *Int J Mech Sci* 1995;37(3):277–95.
- [54] Soldatos KP, Messina A. The influence of boundary conditions and transverse shear on vibration of angle-ply laminated plates circular cylinders and cylindrical panels. *Comput Methods Appl Mech Eng* 2001;190:2385–409.
- [55] Messina A, SKP. Ritz-type dynamic analysis of cross-ply laminated circular cylinders subjected to different boundary conditions. *J Sound Vib* 1999;227(4):749–68.
- [56] Qatu MS. Accurate equations for laminated composite deep thick shells. *Int J Solids Struct* 1999;36(19):2917–41.
- [57] Qatu MS, Asadi E. Vibration of doubly curved shallow shells with arbitrary boundaries. *Appl Acoust* 2012;73:21–7.
- [58] Asadi E, Wenchao W, Qatu MS. Static and vibration analyses of thick deep laminated cylindrical shells using 3d and various shear deformation theories. *Compos Struct* 2012;94:494–500.
- [59] Ferreira AJM, Castro LM, Bertoluzza S. A wavelet collocation approach for the analysis of laminated shells. *Compos Part B: Eng* 2011;42:99–104.
- [60] Ferreira AJM, Carrera E, Cinefra M, Roque CMC. Analysis of laminated doubly-curved shells by a layerwise theory and radial basis functions collocation accounting for through-the-thickness deformations. *Comput Mech* 2011;48:13–25.
- [61] Tornabene F. 2-D GDQ solution for free vibrations of anisotropic doubly-curved shells and panels of revolution. *Compos Struct* 2011;93:1854–76.
- [62] Qatu MS, Rani WS, Wenchao W. Recent research advances on the dynamic analysis of composite shells: 2000–2009. *Composite Structures* 2010;93(1):14–31.
- [63] Liew KM, Zhao X, Ferreira AJM. A review of meshless methods for laminated and functionally graded plates and shells. *Compos Struct* 2011;93:2031–41.
- [64] Fazzolari FA, Carrera E. Advanced variable kinematics Ritz and Galerkin formulation for accurate buckling and vibration analysis of laminated composite plates. *Compos Struct* 2011;94(1):50–67.
- [65] Fazzolari FA, Carrera E. Thermo-mechanical buckling analysis of anisotropic multilayered composite and sandwich plates by using refined variable-kinematics theories. *J Thermal Stress*, in press.
- [66] Fazzolari FA, Carrera E. Coupled thermoelastic effect in free vibration analysis of anisotropic multilayered plates by using an advanced variable-kinematics Ritz formulation. *Eur J Mech Solid/A*, in press.
- [67] Fazzolari FA, Carrera E. Free vibration analysis of sandwich plates with anisotropic face sheets in thermal environment by using the hierarchical trigonometric Ritz formulation. *Compos Part B: Eng*, in press.
- [68] Carrera E. Multilayered shell theories accounting for layerwise mixed description, Part 1: Governing equations. *AIAA J* 1999;37(9):1107–16.
- [69] Carrera E. Multilayered shell theories accounting for layerwise mixed description, Part 2: Numerical evaluations. *AIAA J* 1999;37(9):1117–24.
- [70] Tsai SW. Composites design, 4th ed., Dayton: Think Composites; 1988.
- [71] Reddy JN. Mechanics of laminated composite plates and shells, theory and analysis. 2nd ed. CRC Press; 2004.
- [72] Jones RM. Mechanics of composite materials. 2nd ed. United States: TAYLOR & FRANCIS; 1998.
- [73] Washizu K. Variational methods in elasticity and plasticity. 1st ed. Headington Hill Hall (Oxford): Pergamon; 1968.
- [74] Fazzolari FA. Fully coupled thermo-mechanical effect in free vibration analysis of anisotropic multilayered plates by combining hierarchical plates models and a trigonometric Ritz formulation. In: Mechanics of Nano, Micro and Macro Composite Structures Politecnico di Torino; 18–20 June, 2012.
- [75] Demasi L.  $\infty^3$  hierarchy plate theories for thick and thin composite plate: the Generalized Unified Formulation. *Compos Struct* 2008;85:256–70.
- [76] Demasi L.  $\infty^6$  Mixed plate theories based on the Generalized Unified Formulation – Part I: Governing equations. *Compos Struct* 2009;87(1):1–11.
- [77] Demasi L.  $\infty^6$  Mixed plate theories based on the Generalized Unified Formulation – Part II: Layerwise theories. *Compos Struct* 2009;87(1):12–22.
- [78] Demasi L.  $\infty^6$  Mixed plate theories based on the Generalized Unified Formulation – Part III: Advanced mixed higher order shear deformation theories. *Compos Struct* 2009;87(3):183–4.
- [79] Demasi L.  $\infty^6$  Mixed plate theories based on the Generalized Unified Formulation – Part VI: Zig-zag theories. *Compos Struct* 2009;87(3):195–205.
- [80] Demasi L.  $\infty^6$  Mixed plate theories based on the Generalized Unified Formulation – Part V: Results. *Compos Struct* 2009;88(1):1–16.
- [81] Robaldo A, Carrera E, Benjeddou A. A unified formulation for finite element analysis of piezoelectric adaptive plates. *Comput Struct* 2006;84(22–23):1494–505.
- [82] Carrera E. Historical review of zig-zag theories for multilayered plates and shells. *Appl Mech Rev* 2003;56:287–308.
- [83] Carrera E. On the use of Murakami's zig-zag function in the modeling of layered plates and shells. *Compos Struct* 2004;82:541–54.
- [84] Demasi L. Refined multilayered plate elements based on Murakami zig-zag functions. *Compos Struct* 2005;70:308–16.
- [85] Demasi L. Partially zig-zag advanced higher order shear deformation theories based on the Generalized Unified Formulation. *Compos Struct* 2012;94:363–75.
- [86] Carrera E, Fazzolari FA, Demasi L. Vibration analysis of anisotropic simply supported plates by using variable kinematic and Rayleigh–Ritz method. *J Vib Acoust* 2011;133(6):061017-1–061017-16.
- [87] Reddy JN. Energy principles and variational methods in applied mechanics. 2nd ed. Hoboken (New Jersey): John Wiley & Sons, Inc.; 2002.
- [88] Ye JQ, Soldatos KP. Three-dimensional vibration of laminated cylinders and cylindrical panels with symmetric or antisymmetric cross-ply lay-up. *Compos Eng* 1994;4:429–44.
- [89] Timarci T, Soldatos KP. Comparative dynamic studies for symmetric cross-ply circular cylindrical shells on the basis of a unified shear deformable shell theory. *J Sound Vib* 1995;187(4):609–24.
- [90] Di Sciuva M, Carrera E. Elasto-dynamic behavior of relatively thick symmetrically laminated anisotropic circular cylindrical shells. *J Appl Mech* 1992;59:222–3.
- [91] Matsunaga H. Vibration and buckling of cross-ply laminated circular cylindrical shells according to a global higher-order theory. *Int J Mech Sci* 2007;49:1060–75.
- [92] Ferreira AJM, Roque CMC, Jorge RMN. Static and free vibration analysis of composite shells by radial basis functions. *Eng Anal Bound Elem* 2006;30:719–33.
- [93] Ferreira AJM, Carrera E, Cinefra M, Roque CMC, Polit O. Analysis of laminated shells by a sinusoidal shear deformation theory and radial basis functions collocation accounting for through-the-thickness deformations. *Compos Part B: Eng* 2011;42:1276–84.
- [94] Qatu MS. Vibration of laminated shells and plates. 1st ed. The Netherlands: Elsevier Academic Press; 2004.